Mass Timber Joinery Design for Digital Fabrication and De-constructability

Nathan Brown

A thesis submitted in partial fulfillment of the requirements for the degree of

Masters of Science in Architecture
(Design Technology)

University of Washington
2023

Committee:
Tomás Méndez Echenagucia
Tyler Sprague

Program Authorized to Offer Degree:
College of Built Environments

Abstract

Interest in sustainable architecture is pushing mass timber to the forefront of the industry, but with it there are still difficulties in addressing topics such as the connections between elements. Traditional timber buildings utilized joinery to create a reversible connection between timber elements. By using modern fabrication and computational analysis we have developed a framework to rapidly prototype timber connections and develop modern design guidelines for mass timber joinery for both design and fabrication.

Through generalization one can develop a system for timber joinery by breaking the geometry down into simple parts. Using a geometric model for timber joints from a mesh derived from a NURBS geometry, we can determine metrics for any joint typology with information such as 'contact area', 'overhang area', and 'milling time' from the interaction between the member faces. A finite element model allows us to make general assumptions about joint weakness by evaluating maximum stress and displacements. Using this data together, we can estimate a joint's advantages in both fabrication and structure.

Using this system, we were able to make a case study to test these strategies to see if design principles can be inferred from the analysis for a specific scenario. We used a scarf joint splicing two beams together as our metric for rapid prototyping. By creating a parametric model for the joint, we were able to quickly create both a simulated model and a physical model to compare benefits and limitations in the joint.

These tools can be used for qualitative analysis between functionally identical joints and can produce metrics to compare each joint. These can help to inform design decisions with knowledge from disparate fields to develop designs that provide solutions for many issues.

Contents

Chapter 1

Acknowledgements

I would like to begin by expressing my gratitude towards my advisor Prof. Tomás Méndez Echenagucia for his outstanding mentorship through the years both for the thesis and beyond. Thank you for providing thoughtful and poignant advice while allowing me to make mistakes and discoveries along the way.

I would also like to thank Tyler Sprague for his insights into how to develop a structural system to test this thesis as well as his feedback on how to interpret the data from the results of the structural analysis.

This thesis would not have been possible without the help of the Turner Construction Company, specifically Joshua Lohr, Sean Beatty, and Renzo DiFuria who advised with expert knowledge on current construction methodologies and issues with the fabrication of modern timber joinery. Through their time and effort, this thesis was able to incorporate years of knowledge in design and fabrication as well as physical testing through the use of their fabrication shop. In addition, I would like to thank Tim Veit and Kevin Skinell for their time creating and assembling the physical setup for the joint tests and the finishing of the joinery itself.

I am also thankful to Teri Randall, Renée Cheng, and the Applied Research Consortium for the opportunities to present and obtain feedback for the work on the thesis.

Finally, I am grateful to my fiancé Richard Thomas, for his continual support as I spent countless hours discussing the problems and potential solutions for each step along the process. His knowledge of project management helped to keep the momentum for the thesis going.

Chapter 2

Introduction

Mass timber as a large scale construction material has grown in popularity over the past few decades as firms begin to adopt the structural material as an alternative to steel or concrete. [Harte, 2017] Mass timber has certain advantages when compared to other materials. Timber acts as a sustainable product due to a variety of properties inherent to the material. As a natural material that utilizes carbon in its metabolic process, wood has the capability to store carbon with the material itself. Different varieties of timber are present across most of the planet, providing local supply chains. The microstructure within the timber itself, timber also has a high structural capacity while using fewer materials, contributing to a lightweight structural material. In addition, mass timber has shown benefits in human health and wellbeing through studies focused on biophilic design. [Demattè et al., 2018] Tactile, visual, and olfactory responses have been observed and research suggests that timber has a calming and comforting effect on its residents. The pliant nature of the material allows for recycling and down-cycling and can easily be re-manufactured into a new form. [Zhang, 2022] As such, mass timber has massive potential benefits as a sustainable material in many regards.

While this focus on mass timber as a structural element resolves issues in embodied carbon and uses renewable materials, it introduces new issues that require further research to mitigate such as fire protection, lateral resistance, and the attachment methods in connections. For each of these issues, the geometry of the connection poses as the main factor when determining the performance. Currently, modern construction resolves these

Figure 2.1: Steel connectors are located at each connection point.(Bullitt Center, Seattle, WA, USA; 2011)

issues through the use of additional materials, such as mechanical fasteners or steel connectors as seen in Figure 2.1. This requires different industries for fabrication and requires additional work on site for installation. These can consist of screws for smaller structures and steel plates and bolts for larger structures. These plates tend to be either painted with intumescent paint for fire resistance or hidden for aesthetic reasons, but require the beam to be cut at the ends, reducing its potential to be reused.

Recent interest in both reuse and reductions in complexity have spurred new research for creating all-wood connections for mass timber structures. Companies from many industries in the built environment are creating prototypes for timber connections, studying the effects that all timber connections have on structural stiffness, fire resistance, and seismic performance. These companies are relying upon innovations through materials and pro-

Figure 2.2: All Timber Connection with intumescent strips for the Heartwood Building (Atelier Jones, TimberLab, Seattle, WA, USA; 2022)

totypes for the connection which have large benefits in specific categories. Intumescent strips inside the connection provide additional fire ratings as can be seen in Figure 2.2. Alternative connection types using combinations of mass timber elements are being explored as seen in Figure 2.3. With a renewed interest in both the material and a growing interest in sustainable alternatives to modern construction, evaluating connections still has a large potential for innovation.

There has also been more recent interest in research fields regarding the study of integrated mechanical attachments for all-wood connections. Integrated mechanical attachments consist of interlocking geometries that rely solely upon the geometry of the material to resist and transfer loads without the need for mechanical fasteners or adhesives [Rezaei Rad, 2020]. These connections use only friction and compression in order to transfer loads between parts in an assembly, allowing for separation. Although these types of connections are usually found in traditional timber structures, different forms or research on the mechanical properties of these connection types have increased viability for the products.

Figure 2.3: All-Wood connection test between CLT Elements for the Framework Building(Lever Architects, Portland University, Portland, OR, USA; 2017)

One potential benefit to the focus on timber connections is the potential for material reuse. As reuse is the best solution for reducing the carbon footprint of the building, finding a solution for mass timber to be reused is of vital importance. [Chen, 2019] If treated correctly, mass timber has some of the greatest potential for reuse when compared to other building materials. With current practices timber could be repurposed by removing the ends of a beam. This effectively reduces the potential span for the member but allows for smaller buildings to continue storing the embodied carbon. This process lends itself towards shorter beams which will eventually lead to beams too short for practical uses. An alternative connection with only integral mechanical attachments could provide a means to create reversible connections, thus negating the reduction of the span. Traditional timber joinery provides such a system and utilizes non-destructive interlocking mechanisms as a way to transfer the load. This provides buildings with a structural system that can be removed, inspected, and reused for future buildings. This thesis improves the tool sets for designing and fabricating high performing and machinable joinery through the use of digital fabrication and computational analysis tools.

2.1 Relevance to Modern Timber Joinery

Mass timber joinery solves many of the issues found in modern mass timber construction. From issues such as scope to embodied carbon, timber-only connections have the potential to significantly improve the benefits already present in mass timber.

Firstly, timber-only connections do not rely upon other industries to produce a product. Timber joinery may require complex milling processes, but all processes can be performed by a single industry or even a single machine. Mass timber industries already have the tools and capabilities to provide these types of joinery with the precision needed for joinery. Relying upon other industries causes issues in allowances, as only the largest allowance can be used. [Kindratsky, 2023] Furthermore, whenever another industry is included in a structure, the scope needs to be shared between the two industries. This can cause issues related to communications and coordination. [Kindratsky, 2023] Timber-only connections resolve these issues, allowing for the design to be managed by one industry and has the added benefit of allowing for mass fabrication of connection in controlled environments without the need for on-site adjustments.

Replacing the connection system with all-wood connections also results in a loss of embodied carbon. With the recent focus on embodied carbon in the building, the built environment has begun to shift towards timber for its benefits in carbon sequestration. Removing steel fasteners in timber assemblies provides an immediate benefit in embodied carbon [Fang and Mueller, 2021] as the manufacturing process for timber connection involves no additional energy when compared to manufacturing for an assembly with steel fasteners. The manufacturing of steel plates, bolts, and nails have a much higher degree of carbon emissions even when including increased timber sizes for timber-only connections.

As a further benefit to the sustainable nature of wood, timber connections almost necessitate a reversible construction process. Due to the connection type and order of assembly for the connection, a connection can be disassembled and reassembled many times. Each element in a connection will provide an axis of assembly, with the final elements providing the key for the connection. By reversing the assembly steps, any integrated mechanical connection can be disassembled. Because of this, joinery systems have the advantage of being replaceable. In traditional Japanese temples such as the Picture Hall in the Yakushiji Complex [Brown, 2014], the structure would be inspected regularly. The structures themselves were built to be decon-

Horizontal Section

Vertical Section

Door Frame (movable)

Door frame arrangement: 1. door post (movable); 2. door frame (movable); 3. door sill; 4. base tie; 5. door post; 6. door frame; 7. brace beam; 8. tie beam; 9. small tenons (top and bottom); 10. door post (stationary); 11. brace beam; 12. wedge; 13. tie beam (movable when wedge removed); 14. column; 15. brace beam; 16. small holes for door frame tenons; 17. door sill; 18. base tie (not movable). (See also Fig. 40.)

Figure 2.4: Diagram showing the components for a door-frame for the Picture Hall in the Yakushiji Complex. The frame uses a lock and key mechanism to hold each member in place while still allowing for deconstruction. (Azby Brown, Genius of Japanese Carpentry; 2014)

structed, as can be seen in Figure 2.4. If one of the members had signs of degradation, the structure around the member would be disassembled, the element would be refurbished or replaced, and the structure would be reassembled. With this system in place, timber members can last significantly longer, with some members lasting hundreds of years.

Other temples such as the Ise Shrine use this concept as a tradition [Adams, 1998], rebuilding the temple every twenty years. Six months after the construction process for the new temple is completed, the old temple is deconstructed, and its non-decayed timber becomes available for repairs of subsidiary shrines. The material lends itself to reuse by providing advantages in both strength and malleability. The wood material can be easily carved and shaped into whatever form is necessary and can even be adjusted on-site through the use of traditional carpentry tools. These traditional
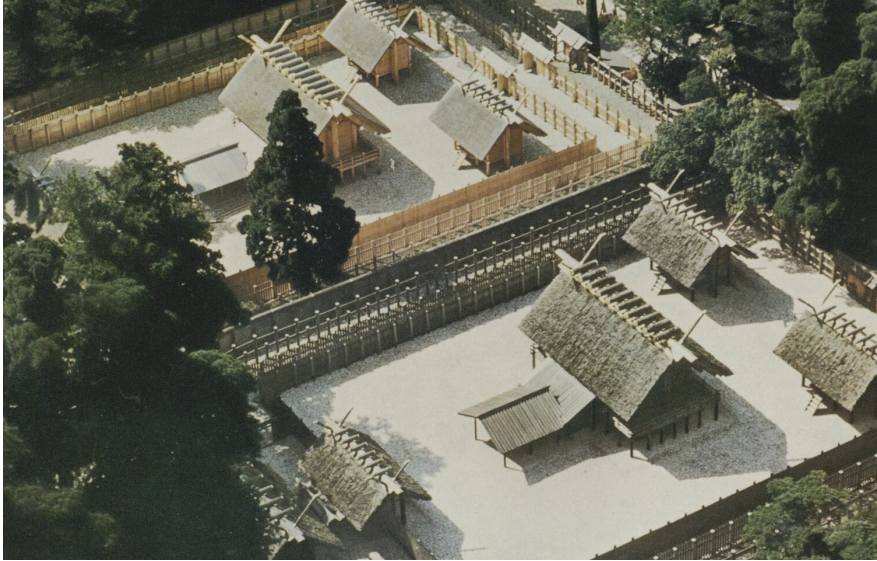
Figure 2.5: Aerial View of the Ise Shrine. Construction of the new shrine can be seen on the left. (Ise Shrine, Japan; 1973)

methods still provide advantages in modern construction, resolving issues in connections quickly and without massive equipment requirements.

2.2   Advantages of Modern Construction

While modern construction has moved away from timber based integrated mechanical attachments, recent technologies provide avenues for reintroduction of these traditional joints. Prior to the industrial revolution, large timber beams and columns were used across the world. As such, timber joinery was developed across different cultures as a way to connect these elements together. With the industrial revolution, building elements began to be standardized and needed a way to mass produce connections. [Moradei et al., 2018] Between the innovations in the manufacturing of standard machine parts, screws, and structural elements, buildings such as the Crystal Palace prioritized steel fasteners over other connections. Steel offered advantages through the simplicity of material, through the moldable

nature of the manufacturing process, and by reducing the scope to one industry. Steel also acted an efficient means of transferring load, requiring only small connections due to its high-strength capabilities. In a location where stresses concentrate such as a connection between elements, this offered distinct advantages. Furthermore, the need for wooden connections for larger buildings was virtually non-existent for most of the 20th century. The popularization of mass timber in Europe in the early 1990s reintroduced timber as a viable product for modern construction. [Harte, 2017] While the knowledge of connections for timber structures has evolved around using steel fasteners similar to steel structures, modern construction now has the capabilities to address the issues in timber-only connections to provide alternatives to steel connections in construction.

Figure 2.6: View of the CNC machine on a track. These tools can be used for large scale milling for mass timber elements such as CLT and Glulam. (Kalisnekoff, Castlegar, B.C., Canada; 2021)

The timber industry already lends itself to both mass fabrication and mass customization. Due to the irregular nature of timber as a product, mills have been incorporating tools that can both mass produce consistent products and implement mass customization. Once timber elements are processed and standardized through the initial milling process, mills utilize computer numerical control machines or CNC machines in order to create customized sizes for beam and columns as well as custom shapes for CLT

or LVL panels with factory level precision. Through the use of digital fabrication techniques such as digital CAM tools, custom connections could be created in an ideal and controlled environment, with little to no loss in the productivity of the machine. Parametric modeling options further lend itself towards mass customization by providing a framework for designing related, but different options. Using parameters to design complex geometries allow for models that can conform to a variety of use cases without sacrificing efficiency.

Timber-only connections provide a unique challenge when assessing their structural performance due to their orthotropic nature. While steel connections require design considerations such as load paths, bolt and screw locations, or the stiffness and shear capacity of the connections, steel as a material behaves in a predictable and relatively simple fashion. Timber on the other hand has the potential to split along the grain, introducing additional issues [Karolak et al., 2020]. As such, steel connections were favored over timber ones for larger construction projects. However, with the advancements in computational power and simulation software, these timber connections can be simulated in a short timeframe, opening up a new avenue for research and development. With this, research on how integrated mechanical attachments function structurally and on where in the joint the forces concentrate are now feasible. These tools can also address the orthotropic nature of the materials and account for the contact elements needed to perform structural analysis on joinery. Parametric design also lends itself to this new age of simulation aided design. By using parametric models, a large design space for a connection type can be tested quickly, allowing for quick iterations and development.

These recent tools in the construction and building industry lend themselves towards a new type of connection. Rather than relying upon a connection that performs adequately in many use cases, connections can be tailored to the specific requirements and changed later. Timber acts as a good candidate for this form of iterative design and modern construction now has the capability to support this.

2.3 Thesis Aims

Timber joinery has the potential to resolve many issues in modern all-wood connections, but a framework does not exist to easily compare different options or quickly settle on the viability of a connection family. In order to

address these issues, we have created a workflow for timber joinery design that considers fabrication and assembly constraints while providing feedback on structural performance and fabrication times. This method allows for easy comparisons between different variations within a connection family with methods for evaluating geometric indicators and comparing them with performance metrics. In order to guide our framework and calibrate our models, we used two case studies of a scarf joint splicing two shorter beams together. For each of the case studies, our model consisted of an assembly supported from below on each end with the splice joint located at the center of the assembly. With this framework, we would be able to provide a baseline understanding of how the connection would perform and narrow the design space, potentially ruling out unacceptable designs and families while validating high performing ones.

Chapter 3

Literature Review

Several factors have prevented timber from being used as a structural material for larger buildings. The natural variability of materials, fire resistance and the lack availability of larger timber members have limited the use of timber as a common material for most of the 20th century. Only with the introduction of mass timber has there been a resurgence in research on timber, specifically on the connections between timber members. All-wood connections are now being sought after as viable alternatives, with research being performed on the structural behavior, fabrication requirements and construction assemblies.

3.1 Material Properties

As a natural material, timber products tend to have varying structural and mechanical properties between not only species but also individual trees or even in the same member. As such, it can be difficult to determine specific properties for timber products, which in turn cause complexity when performing research. While many advancements in categorizing different grades of wood and the creation of engineered lumber have helped to alleviate this issue, the structural performance of the timber still relies upon non-destructive testing and visual evaluation to determine grade [Yang et al., 2008]. As such, research on timber requires large numbers of physical tests to verify results [Karolak et al., 2020] [Karolak, 2021]. This restricts innovation and causes challenges both for research and implementation of timber products.
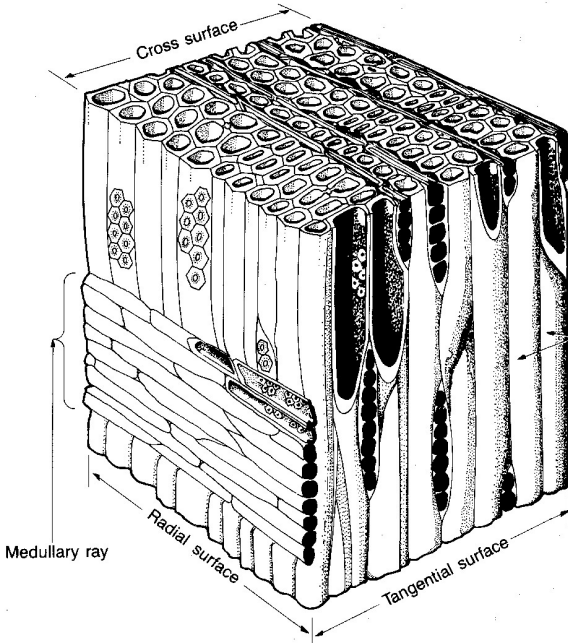
Figure 3.1: Microstructure of softwood material showing the Tracheids and Medullary Rays (Timber Queensland, Australia, 2015)

To further compound the issue, the material properties of timber introduce their own challenges. Unlike common industrialized materials such as steel, which act similarly along every axis, timber has anisotropic qualities also known as orthotropic qualities [Mackerle, 2005]. The structural qualities of the timber differ along each of the major axes of the tree: longitudinally, tangentially, and radially. This is due to the directions the cells run in the natural material as can be seen in Figure 3.1. While some radial cells and tangential cells can be found in the timber itself, the majority of cells run parallel to the grain. When loaded longitudinally (along the grain), wood can resist stresses roughly 20 times larger than when loaded radially (perpendicular to the grain). The properties of the timber along each axis contribute to the overall stiffness and strength of the member.

Mass timber itself consists of a series of smaller timber elements connected together through some fastener, whether it be dowels, nails, or glue.

The timber material generally consists of softwoods, specifically spruce or Douglas fir. When selecting a material for the purposes of a comparative design study, we determined that using the properties of Douglas fir glue laminated beams would provide enough accuracy for the study. Looking at existing literature, rough approximations for Douglas fir glue laminated material properties were found. While the variances in materials would have an effect on the model, the analysis will not require such precision in order to determine trends and design guidelines. Based on the range of values found in the literature, we determined a conservative average for use in the analytical model which are listed in table 3.1 [Kretschmann, 2010], [Vardaxis, 2014], [Langum et al., 2009].

Properties	Literary Range	Variables Used
E-Modulus L	7-16 GPa	11 GPa
E-Modulus T	0.3 - 0.5 GPa	0.4 GPa
E-Modulus R	0.5 - 0.9 GPa	0.7 GPa
Poisson Ratio LT	0.4 - 0.6	0.535
Poisson Ratio TR	0.4 - 0.6	0.419
Poisson Ratio LR	0.019	0.019
Friction	0.4 - 0.6	0.5
Density	400 - 500 kg/m^3	498 kg/m^3
Allowable Stress	11 - 14 MPa	13.8 MPa

Table 3.1: Orthotropic material properties for Douglas fir from Literature

3.2 Finite Element Analysis with Timber

Some studies focus on using simulations to perform structural analysis on all-wood connections. Many of these papers focus on either a specific joint or on a specific aspect of a joint rather than comparing different joints together.

When evaluating the structural performance of an assembly, multiple methods of investigation are often used to validate results and better approximate behavior. When performing research on mortise and tenon joints, Fang [Fang and Mueller, 2021] studied the rotational stiffness of the assembly by creating a numerical, experimental, and physical model to compare to each other. She states that each form of testing requires at least two of the listed models for verifications and performs all three for the joint in

question. Each form of analysis acts as a form of checks and balances by comparing different techniques together. The study focuses on using this validation to create an ease of adoption for structural engineers by verifying that each method produces reliable results. When simulating the mortise and tenon joint in the model, contact elements were introduced in order to transfer the loads between the members in the assembly.

Other studies highlight the effect of the geometry when affected by mechanical fasteners such as [Kunecky et al., 2015] and [Patalas et al., 2022] or with wooden dowels such as [Mehra et al., 2021]. These studies focused on creating a finite element analysis or FEA model of the connection, including either a metal or wooden pin as the primary material to transfer the load. The analyses generally compared the performance of the spliced members to a solid beam, giving a percentage of efficiency for the beam itself. While these studies create FEA models for joint typologies, the effects of the pins and metal fasteners on the geometry itself tended to focus the stresses on or near the contact between the two materials. As such, the geometry of the connection had less of an impact on the outcome than the fasteners themselves. The process itself introduced the same steps as what would be required for traditional timber connections without fasteners.

Others still have focused on the keys and wedges within the model themselves. Sangree et al. studied the effects of key rotations upon stop-splayed scarf joints [Sangree and Schafer, 2009]. They found that the stiffness of the joint and its ability to transfer tension corresponded to the treatment of the key inside the geometry. The direction of the grain in the key itself affected the performance the most as long as the key was not allowed to roll within the joint itself.

3.3   Digital Fabrication in Timber

The tools of construction have always dictated the process and geometry of the connection itself. Traditionally, axes and chisels defined the geometry in timber joints, with sharp interior corners and planar connections. Incorporating timber connections into modern construction brings about a series of new interactions between different fabrication and assembly techniques. Many manufacturing companies are beginning to utilize robotic arms to create prefabricated timber-only assemblies that can be performed with factory precision. Addressing these processes brings about new opportunities, requirements, and restrictions to the design process itself. The allowances between the different members need additional considerations, as the compo-

nents need to fit tightly into place without the use of impact forces. Rogeau et al. utilizes a parametric model for the purposes of testing the different effects the geometry has on the assembly process for through-tenon timber joints with laminate veneer lumber panels [Rogeau et al., 2021]. By examining the angle of the through-tenon, the allowances of the tenon itself, and a chamfer to help guide the tenon in, they were able to create geometry that requires minimal sensors and without the need of a machine learning model. In addition, the design process included consideration for 3-axis and 5-axis milling, evaluating best case scenarios for each. While this technique applies only to the assembly of through-tenon panels, it illustrates that decision on the geometry of the connections early in the design process can resolve issues with fabrication and assembly without resorting to complex and expensive workarounds.

3.4 Timber Connections

Rather than focusing on the application and performative qualities of timber joinery, a number of existing works focus on the parametric aspects for timber joinery. These forms of research rely upon either traditional precedents or upon a parametric tool. Many studies rely upon the existing knowledge already present in traditional architectural models as many Chinese and Japanese temple have timber connections that have lasted hundreds of years [Brown, 2014]

Parametric tools provide a quick and effective means for both educating a designer on the limits and problems of a specific model as well as provide feedback for quick iterations. Larsson et al. create a program called Tsugite in order to test this approach [Larsson et al., 2020]. The software they developed involved a user interface that displayed a voxel based geometry for a furniture joint. Each voxel in the assembly was keyed to a specific member, with users being able to change the geometry by adding or removing the voxels from a specific member. This allowed them to easily assemble a large design space and test different configurations while providing real-time feedback to the users on topics such as fabricability and strength.
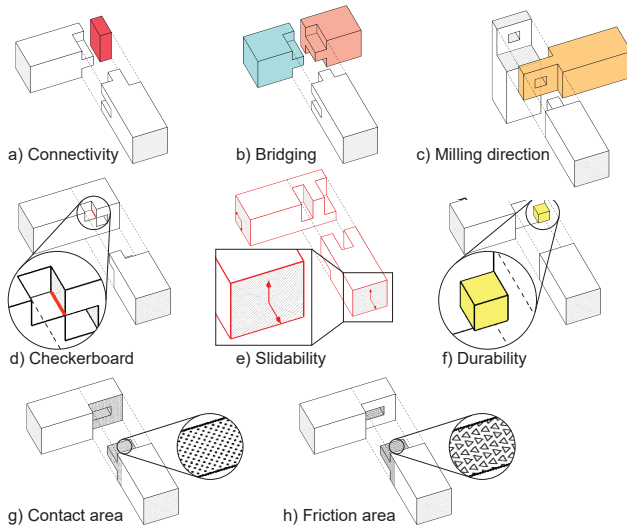
Figure 3.2: Simple metrics were used to evaluate and provide feedback for users when interfacing with the joinery designs. (Tsugite, Larsson et al., 2020)

When creating the tool for the creation of wooden joints, they established geometric criteria to evaluate their assemblies such as contact area, friction area, as well as fabrication constraints such as checkerboards and connectivity as can be seen in Figure 3.2. Because the program also creates the tool-paths for the geometry created, they included fabrication metrics that inform the user that the part cannot be milled. By incorporating a digital tool with a CNC mill, they can transition the design and creation of the connection from bespoke joints to a connection family. However, because they use a voxel based approach to creating joints, they do not include most geometries that are traditionally used when creating furniture or structures. While it does provide benefits in exploring a specific design space, the large variations in the number of connection types and typologies of the joints limits how comparable the joints themselves are. Additionally, this restriction does not take advantage of the centuries of research on effective joint geometries or allow for functionally equivalent geometries to be compared. Furthermore, the study uses the metrics gathered as indicators for performance rather than performing analysis to determine performance. As

such, the recommendations on structural performance depend on measuring areas of geometry with overhangs perpendicular to the grain, limiting their reliability. A system that can determine the performance using simulations would require more computation time but could lead to new insights for design.

3.5 Research Direction

While many studies focus on a specific aspect of the structural or fabrication performance, it can be difficult to extrapolate design principles and general knowledge of timber joinery from these studies. Many of these papers have demonstrated that a computational approach has the potential to demystify these general joint typologies. Applying these studies together through a large design space could yield general knowledge about families of joints while still accounting for the fabrication, construction, and structural needs of the timber. Moreover, comparing families of functionally identical connections allows for designers to still use a design space and weigh the benefits of each connection according to their priorities while seeing how each will perform and what options yield more robust results.

Chapter 4

Methods

4.1   Introduction

In order to address many of the issues found in all-wood connections in modern construction, we needed a framework that could quickly address and iterate on the information from different perspectives. For this study we focused on structural and fabrication perspectives. Understanding timber connections by examining a single joint only provides limited and specific information about that connection and load type. While creating a system that could address all possible load and connection types remains infeasible and would provide limited useful information, establishing a framework to compare similar connection types with the same load enables useful comparisons between metrics. Similar to life cycle assessments, establishing a process for comparing functionally equivalent timber connections allows for rapid prototyping with quantifiable metrics. For this thesis, we defined and tested a framework for analyzing timber connection methods using integral mechanical attachments that addresses many of the issues with timber joinery in modern construction.

4.2   Framework

Modern construction methods tend to avoid these attachment types due to a variety of issues. Before we could create an effective framework, we required a method that resolved most of these issues. From literature, we

found that the primary barriers were a lack of knowledge on structural performance during a typical vertical loading condition, difficulty in manufacturing, and issues regarding resisting fire. [Fang, 2020, Kunic, 2021] While understanding fire remains outside the scope of this thesis, manufacturing analysis and structural analysis are both topics that have received a large amount of attention in recent years. As such, our framework included both topics as metrics that could be used to inform additional design decisions for the design process for a family of functionally equivalent connections. The pipeline we developed included a series of steps which can be seen below: model limitations, parametric connection design, assembly analysis, structural analysis, manufacturing analysis, and metrics as seen in Figure 4.1. This created an iterative process where design of the connection used information from the model limitations and the three sets of analyses in order to find design principles that were prevalent for that family of connections.
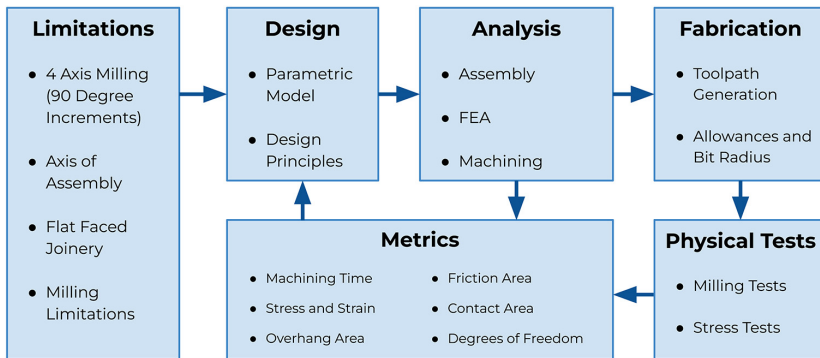
Figure 4.1: The proposed framework for developing and analyzing a set of joint configurations

Each analysis used the parametric model created for the design of the connection to perform their own tests. The analysis for assembly determined the connection type, the contact between the faces, and the degrees of freedom each member had. The structural analysis used the model and the connection results to create a FEA model, simulating the effect of vertical loads on the connection. The manufacturing analysis used the model and the connection results to determine whether and how each part of the assembly could be milled and the time required to manufacture them. The results from these three sets of analysis could then be combined to create

22

the metrics for the permutation.

The feedback loop could either be created manually or through the use of an algorithm. For the manual interpretation of the results, a dashboard helped display different permutations of the designs in the design space, highlighting various attributes and revealing commonalities and differences in the connection design space. From this we could create correlations between geometric indicators such as friction area or joint sizes and performance for the three different forms of analyses. Using an automated approach such as a machine learning algorithm, we could instead easily find what combination of parameters in our connection design performed the best for that specific case. While this would not reveal trends, it could quickly find a high performing solution.

4.3   Model Limitations

As the framework is intended to develop and test designs for timber connections for the built environment, the designs themselves need to be rooted in the system already established. Because of this, a series of constraints were imposed prior to the design process to limit the scope of the design space to only produce feasible results. These constraints take into consideration both structure and fabrication restrictions and limitations.

Firstly, the system needs a clear definition of a connection as well as the elements within the connection. A connection or joint consists of a series of elements or members which utilize an attachment type in order to remain in contact while transferring loads. For the purposes of this framework, the connection uses integrated mechanical attachments as its attachment type. This means that the connection uses geometry and friction as its way of keeping the connection together rather than fasteners or adhesives. Each connection requires at least two members with geometry both outside and inside the connection region. In addition, these members are required to have at least one region that is in contact with some other member. A member is defined as a closed geometry that enters the connection region and is in contact with at least one other member. The member itself does not necessarily need to have geometry outside the connection region. In these instances, the member generally performs a function in the connection such as a key or wedge. Because these elements are all timber elements, each member requires grain direction, which normally corresponds to the member direction. This grain direction is used in subsequent analysis tools to determine the milling capacity.
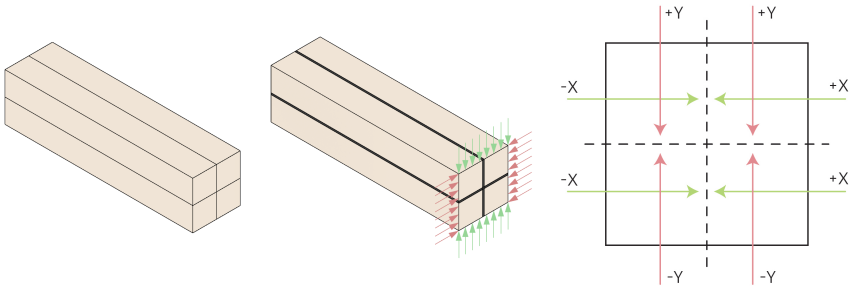
Figure 4.2: Each member could only feasibly be milled from each side, restricting the milling process. In order to maintain a high accuracy when milling connections, the milling process only reaches halfway into the member from each side.

Fabrications considerations for the members in the assembly were required based on restrictions specific to the fabrication process. As such, there are a series of rules that need to be adhered to for the study. Because we are primarily dealing with linear elements rather than plates, the milling process for the elements will utilize some form of milling from the 4 axes perpendicular to the grain direction. For the purposes of the study, we utilized fabrication machines with a bit rather than a saw. To maintain accuracy, the depth of the cut were restricted to half the depth of the members, as milling with longer bits introduces inaccuracies and require larger tolerances. When performing the analysis for these parts, milling bit access and depth were taken into consideration and baked into the analysis process. Additional work could be done to make this framework either include alternative fabrication processes or panel shaped elements such as CLT, but that was beyond the scope of the study.

The final considerations required for assembling the design space was the use of planar geometry for each of the members. This restriction simply meant that no design spaces with curved surfaces could be explored. This was not only used because the analysis process used a mesh rather than a NURBS surface, but also because this more closely reflected traditional joinery, allowing us to compare simulated results with existing typologies. From an assembly and fabrication perspective, the planar surfaces generally produced more valid design spaces, further supporting the restriction.

4.4   Connection Design

In order to create a connection design model for the framework, functional equivalence first needed to be established. This allowed for each of the connections in the design space to be compared without qualifications. As different connections would experience different forms of bending, shear, and other stresses, this necessitated that model definition remains the same. Member sizing, assembly components, wood species, and loading cases acted as the model limitations for these connections. For member sizing, the limitations imposed were member height, member width, and member length. As both the size of the member and its span can affect the bending and shear, the size needed to remain equivalent. Similarly, the species of wood was restricted to one type for the purposes of the study: Douglas fir. When designing the connection itself, the number of connections and the assembly directions determined how the joint performed and thus needed to remain the same. Finally, due to the complexity of the model itself and the static nature of structures, only a single vertical load case was considered, determined by a typical loading of that connection family. By creating these restrictions, the connection family being tested could be evaluated without introducing additional complexity.

In addition to the model limitations, other factors affected the design. Because this study focused on fabrication and manufacturing, additional fabrication constraints were imposed. These included access for the machining bits, planar faces when machining, and degrees of freedom for the assembly process. With these fabrication constraints considered, a parametric model would allow for different variations on geometry while still creating a comparable design space. For the purposes of the study, we created parametric models with manually imposed limits on parameters rather than procedural ones. The parametric models were created using Rhino 7 as well as a Python script and a Grasshopper interface for generating the geometry.

4.5   Connection Analysis

As part of the computational approach to the design of timber joinery, a series of analysis tools were developed to determine the performance of the connection. The first of which evaluated the connections themselves, evaluating how the members were assembled, the directions of the members, and what parts interacted with each other. Using inputs from the parametric model, such as the geometry and the number of members in the assembly,

the geometry would need to be converted into a graph or node map so that other software could perform the analysis. We selected COMPAS, an open source Python meshing package [Mele and many others, 2021], as our meshing software, which could receive vertex and face information, converting it into a class that could then be further modified with methods that could access neighbors and intrinsic properties of the geometry such as face normals or centroids. COMPAS also allowed for integration with other packages such as with COMPAS_Vibro, enabling us to export the mesh to other programs for the structural and fabrication analysis.

Before analyzing the connection itself, each member needed to be evaluated individually. For the purpose of determining the general information on the member direction and size, we first converted the geometry into a mesh for each member. Assuming that the member would take the form of a typical rectangular prism, the set of faces not coplanar to the bounding region would form the joint region. This information was then used as the baseline for determining the assembly and sliding directions for each of the members.
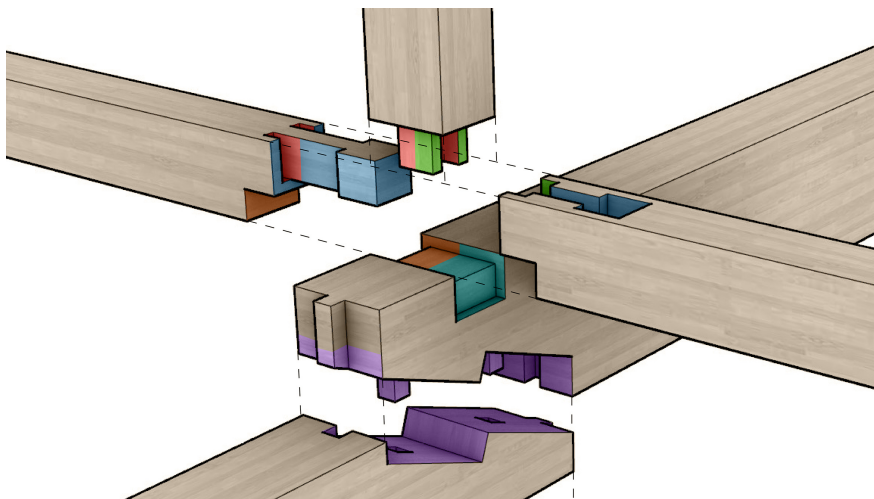
Figure 4.3: Diagram illustrating an example assembly. Connection Analysis finds contacts between different elements in the assembly. Each color is associated with an element pairing.

To understand how the assemblies would be milled and connected, we first needed to establish what faces contact each other and how the assem-

bly could slide and move as a whole. This provided valuable information for other forms of analysis, but also metrics in the form of contact and friction area. Contact between members was established for both faces and edges between every member pairing. To find the contact faces between two members, each face pairing was compared to evaluate if each were coplanar to one another. If the two were coplanar, the ends of the edges were compared to discern if and where the faces overlap. Once performed for all face and member pairings, we effectively could know each member's contact information as can be seen in the example in Figure 4.3. We used a similar process for edges which involved collinearity instead. When gathering the metric for contact area, we calculated the overlap between the faces rather than taking the face area, due to some faces contacting only parts of other faces or multiple faces at once.
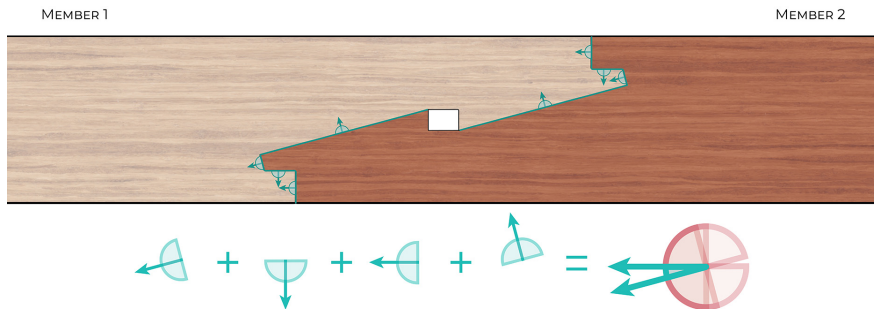
Figure 4.4: Diagram illustrating how face normals restrict movement and how summing face normals results in finding unrestricted axes for disassembly.

Once the contact faces were established, discerning whether the faces were able to slide past each other was a simple matter of finding the face directions for the contact faces. When two faces from different members are in contact with each other, they restrict the movement of the two members in the assembly. For each face in contact with a member, its face normal restricts the movement based on the dot product of the sliding direction and the face normals. If the dot product for all contact faces remains positive for a particular sliding direction, the part can slide along that direction. An example can be seen in Figure 4.4. For the purposes of the study, rather than find every potential vector for assembly, we utilized a system that only evaluated sliding direction rotated around the three local Cartesian coordi-

nates based on the direction of each member. By using the dot product of the vector, we could construct a range of rotations with positive dot products for the face normals. From this, we would output the minimum and maximum vectors for the sliding range. While this excluded many potential vectors, this approach supported the fabrication approach we would be utilizing. This process also does not consider all possible assembly options, such as assembly directions with multiple steps per part. While the process does not perform an exhaustive approach, when evaluating traditional joinery geometries, the could quickly and reliably find the only initial sliding directions for disassembly.

Finding the potential axes of assembly not only determines the potential for assembly, but also could be combined with the contact faces to calculate the friction area between each pair of parts in the assembly. The assembly information gathered during this method would then be used in subsequent steps, specifically mesh sizing for structural analysis, for sliding face allowances during manufacturing, and for rounding exterior edges which have an equivalent interior edge on another member for the purposes of fabrication.

4.6   Structural Analysis

The structural performance of the connection was calculated by utilizing a simulated model to estimate the stresses that would be found during a typical load case for the assembly. FEA models generally study the effects of forces on geometry for a variety of applications from acoustics to structural performance. The method utilizes a discretized mesh and input loads to understand how the member reacts. It determines how each element in the model resists the loads, taking into account its material properties. Generally, designers use guidelines for structures early in the design process to evaluate different designs. While this functions well for structures, the complex geometry inside of timber joinery causes portions of the joint to behave unpredictably. For this reason, FEA provides a robust and flexible model for estimating the performance and comparing different connections types to each other. Due to the comparative nature of the study and the number of comparisons we wanted to investigate, we elected to only use a static linear analysis with limited contact areas to avoid further convergence issues.

When simulating structural performance of mechanical attachments for timber elements, the FEA model requires the use of orthotropic materials

as can be seen in Figure 3.1. Timber as a material is composed of a complex microstructure. The timber itself has different elements: radial cells, longitudinal cells, with lignin acting as a glue between the cells. The longitudinal cells form the bulk of the material and create the grain, while the radial cells hold the longitudinal cells together and resist shear. Together this forms a material that is strong along the grain while being weak in the radial and tangential axis. In addition, knots and warping in the wood will change the grain direction and thus the material properties. In order to simplify the model, the material was assumed to be a perfect orthotropic material, with the highest elastic modulus being aligned to the longitudinal direction of the member in the assembly [Vardaxis, 2014]. For this process, we used ANSYS Mechanical APDL, as the program had the capabilities to perform static linear analysis on orthotropic materials using contact elements. From the FEA model, we calculated the displacements as well as the principal stresses from the model and used their magnitudes to determine the overall performance of the connection as well as where the largest stresses were located.

In order to interface with ANSYS, we used COMPAS_Vibro, an open-source package developed for Python [Echenagucia, 2020]. Originally used for acoustical modelling, COMPAS_Vibro integrates with other structural analysis software, allowing a COMPAS mesh to be imported and tested in an FEA software. The package does this by converting the mesh into an input file in the format suitable for the API of the FEA software, including data such as loads, supports, and material properties. The package then receives the result and formats the response in a readable format such as a JSON file.

4.6.1   Meshing for FEA Analysis
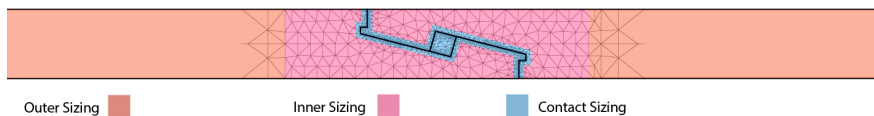
Figure 4.5: Diagram of different GMSH sizes. Finer sizes in the joint region and in the contact area are highlighted by different colors.

In order to properly analyze the structural performance of the assembly, we first needed to discretize the mesh into smaller, more regular elements. A re-meshing tool is generally used for these purposes, dividing up each face of the model into small, uniform elements. We selected GMSH as our remeshing software, as it had the capabilities of creating a solid mesh while allowing for refined meshes in specified regions. As an open source Python package, GMSH was able to use the COMPAS mesh generated in the previous steps and output a series of tetrahedrons divided at even intervals that could then be imported back into a COMPAS mesh [Geuzaine, Christophe and Remacle, Jean-Francois, 2020]. The meshing algorithm attempts to create a mesh with as many regular tetrahedrons as possible, using the mesh size given as the basis for the edge length. The result was a solid mesh that contained the same geometry as the original COMPAS mesh, but comprised of tetrahedrons at specified sizes.

Mesh sizing was controlled based on a series of tests of the members based on performance. Finite element analysis does not produce the same results for all mesh sizes. As a general rule, smaller mesh sizes lead to a reduction in stiffness, but tend to produce more accurate results. The reduction in mesh sizing tended to converge on a specific stress, where additional reductions in mesh sizing produced negligible changes in the performance of the assembly. In addition, because the study focused on the joint region itself rather than the entire assembly, a smaller mesh sizing was used for the half of the beam that contained the joint region as seen in Figure 4.5. For the finer mesh sizing, a region encompassing every joint region within the joint family was used to maintain the same mesh sizing across the different permutations in the connection typology. Having a smaller mesh size for only a portion of the assembly provided more reliable information without requiring additional computation time for areas of the assembly without complex geometry. Similarly, contact areas for FEA models needed fine mesh sizing in order to properly calculate intersections between contact faces and allowing the simulation to converge in a reasonable timeframe. A finer mesh size was applied to any face found to be in contact with another during assembly analysis.

In order to achieve a reliable result without requiring fine mesh sizes to be used across the entire assembly, a series of mesh sizes for each section were tested. After running the tests, each mesh size was compared to the next sizing to calculate the change in stress across sizes. The mesh size combination with the largest size and minimal change across both mesh sizes was chosen for each member size as seen in tables 4.1 and 4.2 (Size combination highlighted in bold). The limitations for the mesh sizing for the

	Outer Sizes					
Inner Sizes	**16 cm**	**8 cm**	**6 cm**	**4 cm**	**3 cm**	**2 cm**
16 cm	24.1					
8 cm	28.4	28.8				
4 cm	31.6	37.1	34.7	35.1		
2 cm	36.5	37.9	39.6	38.4	39.3	39.8
1 cm	39.7	44.3	43.1	42.9	43.7	44.2
0.75 cm	40.0	43.9	44.2	**44.2**	44.9	45.3

Table 4.1: 10 cm x 10 cm Beam GMSH cell sizes, comparing sizes near the joint region (Horizontal) and sizes outside the joint region (Vertical). The stress results (GPa) were compared to find a size combination with minimal cell counts while having few changes in stress.

	Outer Sizes					
Inner Sizes	**32 cm**	**16 cm**	**8 cm**	**6 cm**	**4 cm**	**2 cm**
32 cm	11.5					
16 cm		22.6				
8 cm		23.8	23.4			
4 cm	35.2	44.2	46.6	48.9	34	
2 cm	48.8	60.5	52.1	46.2	42.1	40.7
1 cm	71.0	64.3	62.9	**65.7**	74.3	71.7
0.75 cm	62.3	63.7	70.7	71.5	71.4	70.5

Table 4.2: 30 cm x 10 cm Beam GMSH cell sizes, comparing sizes near the joint region (Horizontal) and sizes outside the joint region (Vertical). The stress results (GPa) were compared to find a size combination with minimal cell counts while having few changes in stress.

ANSYS student license was 50,000 elements, which restricted the inner mesh sizing. Around the contact area, the smallest mesh sizing was one quarter the size of the inner mesh size, with a fall-off distance of half the inner mesh size. This increased the convergence rate for the simulations without sacrificing overall mesh size or accuracy. With these settings in place, a reliable model was constructed for each permutation, outputting vertices, faces, and tetrahedrons, with additional capabilities for slight changes to the meshing when issues with convergence occurred.
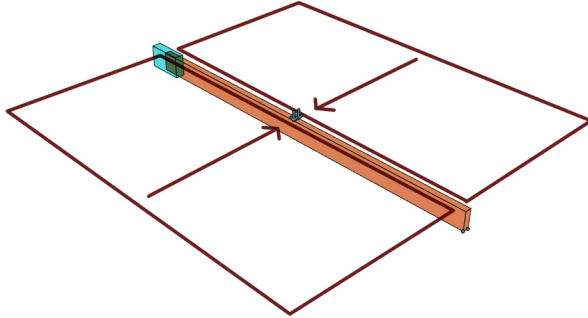
Figure 4.6: An example FEA setup for ANSYS. The framework only placed loads on the horizontal members and determined the weight through the use of a tributary load for typical dead and live loads.

4.6.2 Loads and Supports

When preparing the permutation for the simulation, the supports and loads applied were placed in the same positions to maintain functional equivalence. A point load was placed in the center of each non-key member in the assembly with a value corresponding to a percentage of the tributary load for a floor above for horizontal members as can be seen in Figure 4.6. The load was distributed across the different points at the top of the beam located at this distance. In order to determine the load for each of the sides, a series of tests were performed for a solid member, finding when the solid member reached its allowable stress. Structural tests would use this value as a baseline, using a percentage of the allowable load both for convergence of the FEA model, and because connections would inevitably have lower load capacities than solid counterparts.

Similarly, the test for the assembly would rely upon supports located at the opposite ends of each member. In order to mitigate reaction forces at the support, a standard pin and roller setup was used for the assembly. One member would be marked as the 'fixed' beam with a series of pins along a line on one corner located on the opposite side of the joint region. An example of a setup for a traditional scarf joint can be seen in Figure 5.3 on page 54. The other members in the assembly would receive rollers along a line similar to the first member. These would only be restricted along the z axis. In order to prevent unnecessary twisting of the members when loaded, additional

32

restrictions were enforced along the sides of each member, preventing it from moving from side to side. With these restrictions in place, the results would provide the stresses for a typical loading case without unnecessary information such as lateral-torsional buckling.

4.6.3 Contact Elements

For the purposes of accurately measuring the effects that the members have on each other and the assembly, automatic contact elements were used. Because timber joinery utilizes integrated mechanical attachments, the two parts use a standard frictional contact that allows for separations rather than a bonded contact. ANSYS developed a function that determines what elements could potentially be in contact with one another and applies the contact type to each part. For this type of contact, ANSYS uses a system similar to springs, in which forces are introduced when two contact elements penetrate each other, with the force directly proportional to the amount of penetration. As the assembly contained many interior corners in the geometry, we needed to include the feature edges when determining contact. With feature edges, interior corners in the geometry provide additional springs to guide elements in the other part back. Due to issues with convergence, the contact penalty for the contact elements was set to 0.1. This did not have a noticeable impact on the stress within the members. While this process introduced complexity to the model and introduced convergence issues, determining the structural performance of the assembly was impractical without contact elements. Because each part of the geometry applied forces based on what other elements they interact with, estimating these forces without contact elements for any geometry could not be achieved.

4.6.4 Performance Evaluation

Once the simulation has applied the forces and converged upon a result, we could use the displacements and principal stresses to evaluate performance. Because the model uses a linear elastic material and because we are interested in qualitative differences in the models rather than accurate estimates, we limited the applied load to a percentage of the expected capacity. This preserved our ability to compare the different joints in the family while maintaining a high convergence rate for the simulation. We extracted the principal stresses for each of the nodes as can be seen in Figure 4.7. From there, we used the maximum principal stress for the assembly and compare them to the other permutations at the same load rather than
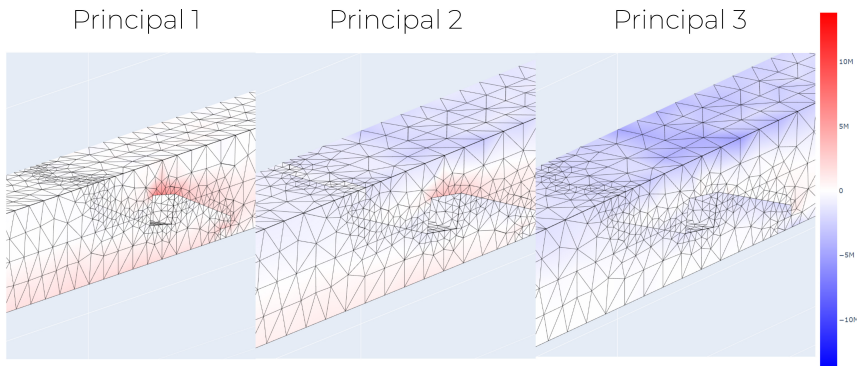
Figure 4.7: Each of the principal stresses provides a local description of stresses in the material. When combined, these forces can indicate the compression and tension in a material as well as the direction

loading them to the allowable stress. When evaluating the data however, we found that some permutations would concentrate the stress into a single element. We found that for the assemblies that tended to concentrate loads, small changes in the mesh sizing or loading could have some impact on the resulting stresses. In addition, as the assembly could receive a local failure, such as the crushing of the grain, and distribute loads to surrounding areas, we elected to create a series of results for stress that could paint a better picture for how the assembly performed rather than just its highest stress.

Culled Load

When looking at the distribution of stresses in the members, different members would perform better or worse depending on the stress at a certain percentile. Some connections would have stresses concentrated at one point, while others would distribute their stresses along the entire joint region. Evaluating the assemblies at different points in the distribution revealed that assemblies that distributed their loads more evenly would tend to have higher stresses overall except at the highest percentiles as can be seen in Figure 4.8. In addition, if the maximum stress was located in a single or few vertexes it would cause a high degree of noise when comparing to other simulations. As such, we determined that the efficacy of the culling method rested in its ability to filter out the variances in the model but

34
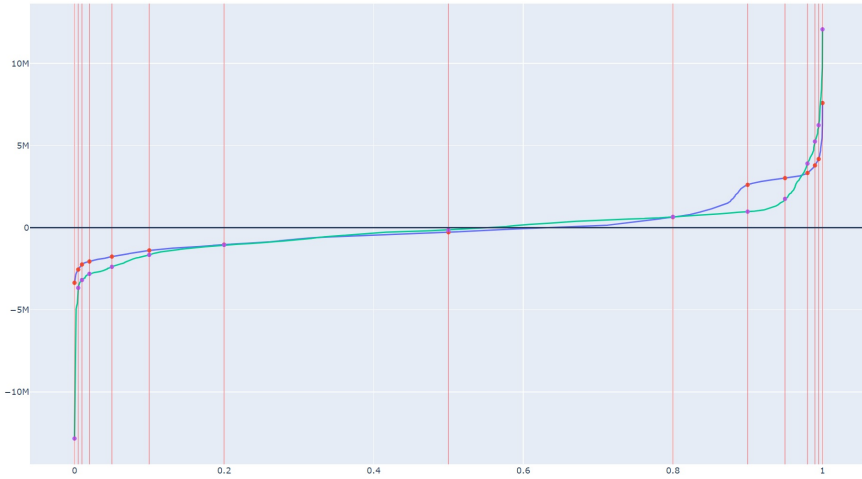
Figure 4.8: Graph showing the sorted stresses for the joint region in the FEA Simulation, displaying the distribution of forces along the vertexes with a high performing (blue) and a low performing (green) model. Selecting a cull percentage can reduce noise while preserving performance differences.

would produce incorrect results if used liberally. High performing assemblies tended to distribute the forces to more vertexes, while lower performing assemblies concentrate the forces. Selecting a high percentage to cull would cause some higher performing permutations to perform worse than their counterparts. Selecting a low percentage of culling removed the variance seen when performing similar tests but preserved the overall trend seen when comparing different permutations together. Because of this a low value of culling provided an effective means for comparing permutations.

Blurred Stress

As an alternative to culled stresses, blurred stresses simulate local failures without removing data. In order to smooth the stresses, each node in the mesh would distribute its load across the entirety of the remaining geometry, using a distribution quantity based on a Gaussian curve as can be seen from the equation below where d is the distance from the node. The distribution is affected by the σ value. This effectively acts as a smoothing effect, removing extremes from the results while preserving total stresses
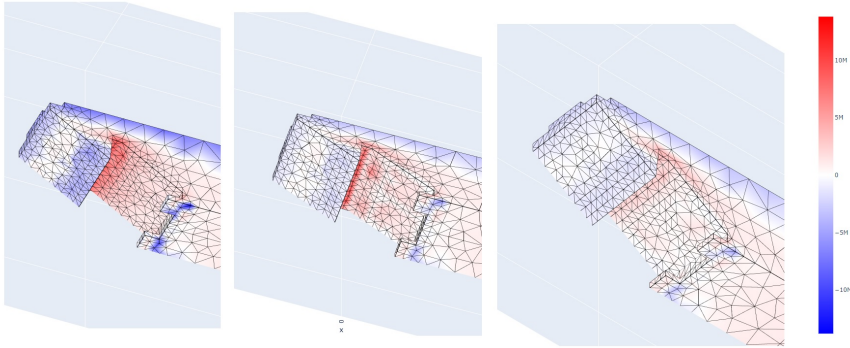
Figure 4.9: Diagram showing force smoothing across different percentages, showing a σ value of 0, 0.0001, and 0.0005

and overall hotspots. While this effect helped to distribute the forces across a larger volume, it did not have a large effect when comparing different permutations together, with the general fitness landscape for performance shifting rather than becoming less noisy.

$$G(d) = \frac{1}{\sqrt{2\pi\sigma^2}} e^{\frac{-d^2}{2\sigma^2}} \tag{4.1}$$

Volume above Allowable Stress

Another alternative to culled stresses was to calculate the volume of the connection that passed the allowable stress of the material. This quantity indicated the magnitude of the failure through material rather than stress itself. While this directly recorded the results we were concentrating on, it heavily biased connections that concentrate their stresses in a single area, without taking into account how much stress existed in these local areas. In addition, this method did nothing to reduce the variances found in the FEA results and was reliant upon the stresses surpassing the allowable stress for the material. Due to the need for low loads for the convergence of the FEA model, some results never surpassed the allowable stress in the model. This method would require further investigation to be used in the framework.

Performance Method Discussion

While none of the alternative methods for analysis produced accurate results, each provided an additional lens for understanding the assembly's performance. For the purposes of the study, we found that the culled values provided a useful series of metrics through the use of the culling percentage. Additional explorations using a similar approach for the other metrics could introduce new metrics for evaluating the assemblies. Many of these metrics could also be reduced down to a single metric, making it a good candidate for analysis or Pareto fronts for additional data interpretation. With the culled stresses and the maximum displacements, we could evaluate trends in the performance of the assemblies in order to find design guidelines for connection design.

4.7 Manufacturing Analysis

While structural performance determined if the connection could meet the structural requirements, modern construction requires that the connection have an ease of manufacturing. Metrics on the manufacturing side of connections fill an equally important role in determining the viability of the connection designs. With the introduction of CNC machining, ease of manufacturing boiled down to what machine was required for the connection, the amount of time on the machine for each part, and the physical labor involved in getting the machine set up and adjusted for the series of cuts. The analysis used the geometry given in the previous steps and the data from the assembly analysis to calculate these metrics while also creating CAM information for the rapid prototyping for physical testing.

4.7.1 Millability

We defined millability as the ability for a 3 axis or 3.5 axis CNC machine to mill a part using a standard bit without the need of additional cuts or manual processes. When evaluating each metric, a 3.5 axis was assumed to only be able to access the part from the sides in ninety degree increments. The 3 axis version could only be reached from a single direction. We divided the process of determining millability into two distinct steps; milling direction and overhangs and evaluated each along each milling axis. By combining these together with the different milling access, we could not only find what geometries could be milled, but also which parts could ben-

efit from milling with the side of the bit and which faces required the head
of the bit to be milled.

Milling Bit Access
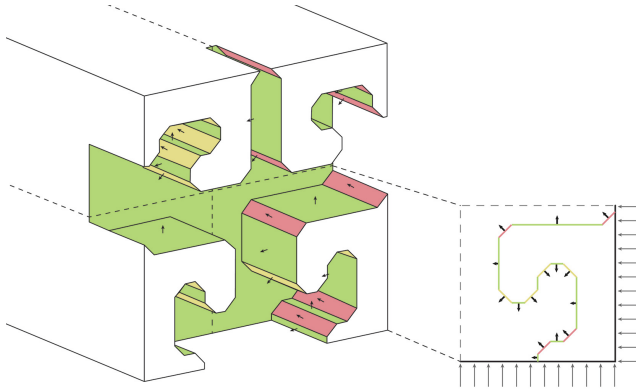
Figure 4.10: Diagram illustrating how the algorithm determines milling bit
access. Faces in red cannot be accessed. Faces in orange can be accessed
but are not orthogonal, and faces in green can be accessed from the head.

Using the geometry of the part, a part could only be milled if the bit could
reach each face within the joint region. For each milling direction, using the
dot product of a face and the milling axis, a number between -1 and 1 can
be found. This number can then be evaluated based on the table 4.3 and
added to the geometry data as seen in Figure 4.10 Additionally, because we
assumed that the bit would not be able to reach past the halfway point in
the member, any face that extends past the halfway point also cannot be
accessed by the bit and would be flagged as not millable.

Value	Result	Priority
$x = 1$	Facing (End Mill Required)	1
$0 < x < 1$	Facing (Ball Mill Required)	2
$x = 0$	Side	0
$x < 0$	Not Millable	3

Table 4.3: Milling Direction Classification Table

Overhangs
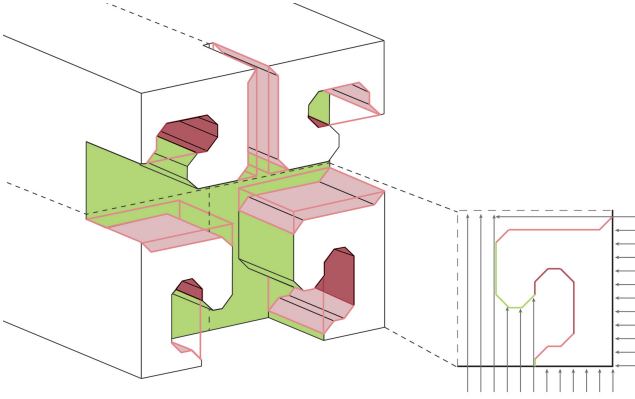
Figure 4.11: Diagram illustrating how the algorithm finds and evaluates overhangs. Faces within the red boxes cannot be accessed due to overhangs.

Similar to the face direction, discovering what faces in the geometry were unreachable due to overhangs required the face direction and face boundary in conjunction with the milling direction. This analysis used the boundary of faces with a negative dot product and projected their boundary to faces with face centroids located below them. The faces were determined to be underneath a face using a similar process for contact between members as described in the assembly analysis section. For this analysis, both faces were projected down to a single plane to analyze the overlap. If a face existed underneath with a non-negative dot product for the face direction, that face wouldn't be able to be milled from that direction.

Multi-Axis Machining

The millability of the connection with a 3.5 axis CNC machine requires each face to be milled from at least one direction. By combining the metric from both processes, we could ascertain if any face could be milled from any of the four directions. Faces are classified based on the highest priority in each direction. Once each face has been evaluated from all milling directions, a determination could be made if the face is millable both from a milling direction and an overhang standpoint. Distilling this down for all faces in the geometry we calculated a millable metric for the geometry as a whole so

(a) Mill Access   (b) Overhangs
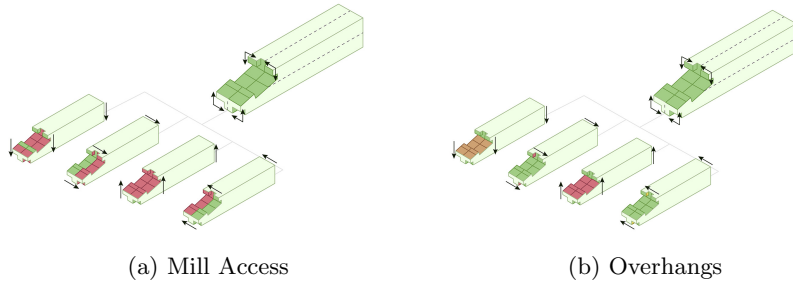
Figure 4.12: Diagrams illustrating how the CNC only needs access to a face from a single direction. Using multiple directions together allows for a larger number of designs to be milled.

that we could quickly disregard permutations in the connection family that could not be milled. We could also use the information from the milling access to prioritize cutting directions for each face.

4.7.2 Milling Curve Creation

To calculate milling time, we first needed to analyze the operations the CAM program would operate for each face in the geometry. For simplicity, we assumed that the CAM program would only perform 2.5 axis operations and use the rotation to turn the part. Creating a series of cuts at different depths for each of the orthogonal directions enabled a larger design space than just evaluating an operation from one direction or relying upon a 4 axis milling operation. These would be created by generating a set of flat curves from a series of depths that would fully describe the geometry as can be seen in the example in Figure 4.13. These curves would then be sent to a milling software to cut out using a pocketing operation. From this we would be able to take the area removed from the operation and the depth to calculate the time for each operation, thus determining milling time for each side.

Before creating the curves, the faces first needed to be organized and sorted into different depths. We organized the faces using the face direction attributes to find face normals perpendicular to the mill direction. Because a perpendicular face could be milled by running a bit along the bottom edge of each face, a set of edges could be created by finding the edges farthest from the milling direction along the face. Combining these edges together
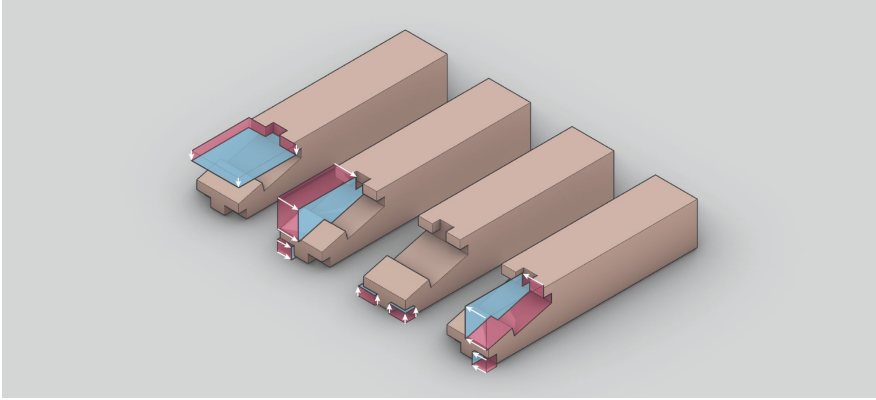
Figure 4.13: Diagram illustrating how each side can define a portion of the geometry and how most geometries can be described by flat curves along each of the four directions.

and sorting the faces based on their depth created a series of curves at set depths for the cuts from that particular direction. From these curves, a script connected the curves created from each face together with a polyline from the components. If a portion of the geometry was reached without a curve to attach to, the script created a polyline along the geometry at a set depth, using the face normals and edges to generate the polyline. This process would repeat, with the curve crawling along the geometry in one plane until the curve reached a face along the outer surface of the member. Once each curve reached the bounds of the joint region for a set depth, the curves would then connect together by crawling along the outer joint region until they formed a closed region in the joint area. This region became the base curve for milling, but still lacked other considerations for milling such as overhangs that would block the bit.

To prevent potential issues with overhangs, each curve would be evaluated against all overhangs to see if a portion of the curve would need to be removed. This process used a method similar to the overhang detector created previously in the millability subsection to check for overlaps. If any were found, the polyline from the overhang was used to perform a boolean operation, only keeping the region outside the overhang. Once the overhangs were removed, additional operations for the milling operations themselves were performed, with allowances being applied to each side. Different allowances were used based on the sliding directions of the assembly. The

41

paired corners found during assembly analysis were then applied, with a fillet for exterior corners created using the bit radius and the allowances. Additional pockets would then need to be created for faces with normals opposite to the milling direction. With these a pocket can simply be created by using the face outline and removing any overhangs from the curve generated.
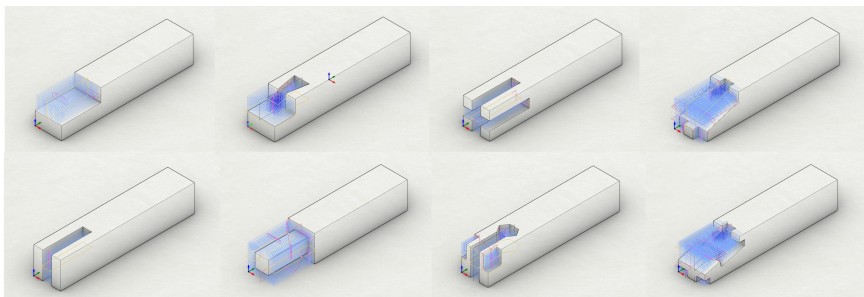
Figure 4.14: The process for creating the curves allows for mass customization through the use of automated milling. The curves created during the milling process also allow for additional parameters such as allowances.

These curves could then be transferred to a CAM software with an API such as RhinoCAM and used to automatically generate G-code for the milling process. The data found from performing the analysis estimates not only if the part could be milled but the milling time and the number of operations the part will take. This process could be repeated for most geometries other than curved geometries and geometries that had oblique faces from all milling directions, which allowed for mass customization in the fabrication process, as seen in Figure 4.14. This process could take into account bit sizes and allowances, creating a more automated milling process while retaining flexibility needed by machinists to create geometries with the tight allowances that are needed.

4.8   Physical Testing

Physical testing calibrated and verified the results from the previous analyses. While the physical testing could not be automated, testing a small sample of the total design space oriented the design and allowed the simulations to produce more realistic results. For each of the physical tests,

Figure 4.15: Setup for the fabrication process. The machine used during this step determines the limitations for the entire framework

we used the available facilities and the materials as the boundary conditions, as these are forming the limitations of our designs. For the purposes of this study, we used a 4-Axis CNC machine as can be seen in Figure 4.15.

For the purposes of the tests, we recreated the loading conditions from the simulation by loading weights gradually and measuring the responses at each weight. An example of the setup for a case study can be seen in Figure 4.16. In order to gather material properties, we first measured a solid member, gradually increasing the load as set weight intervals. At each stage, the displacement of the members could be measured using an analogue indicator tool to measure up to a 0.003 cm difference. To create an accurate comparison between solid elements and timber connections, we loaded the solid element for its material properties before cutting the member and creating the assembly. Using this method, we could compare the performance with the same material, thus mitigating the impact of different timber elements having differing structural properties. In addition to loading the assemblies

Figure 4.16: Setup for structural testing

and testing for deflection, we loaded the assemblies to critical failure and recorded the locations of failure, comparing them to the simulations.

With this information, we could calibrate the simulations by finding the material properties that most closely match the data. In order to quickly test the different materials, we ran the simulations through a Genetic Algorithm or GA. This GA received the material information, such as the elastic modulus, the Poisson ratio, and the density as variables and simulated the solid element loaded at each of the loads recorded to optimize the material. The GA then compared the resulting deflections from the loads and attempted to find the material properties that most closely match the results from all the load cases. These results were then used for the subsequent simulations.

From this, we compared the physical testing data with the simulation data to determine the accuracy and precision of the simulation and see if the simulation acted as a good indicator for high performance. This process created a check and balance system for the entire framework, rooting

the simulations within reality and calibrating the models. While the study focused on the fabrication and structure of the assembly, additional tests could be performed as needed to produce additional metrics or further refine the simulation.

4.9 Metrics

(a) Contact Area

(b) Friction Area

(c) Degrees of Freedom

(d) Maximum Stress

(e) Displacements

(f) Millability

(g) Milling Time

(h) Overhang Area
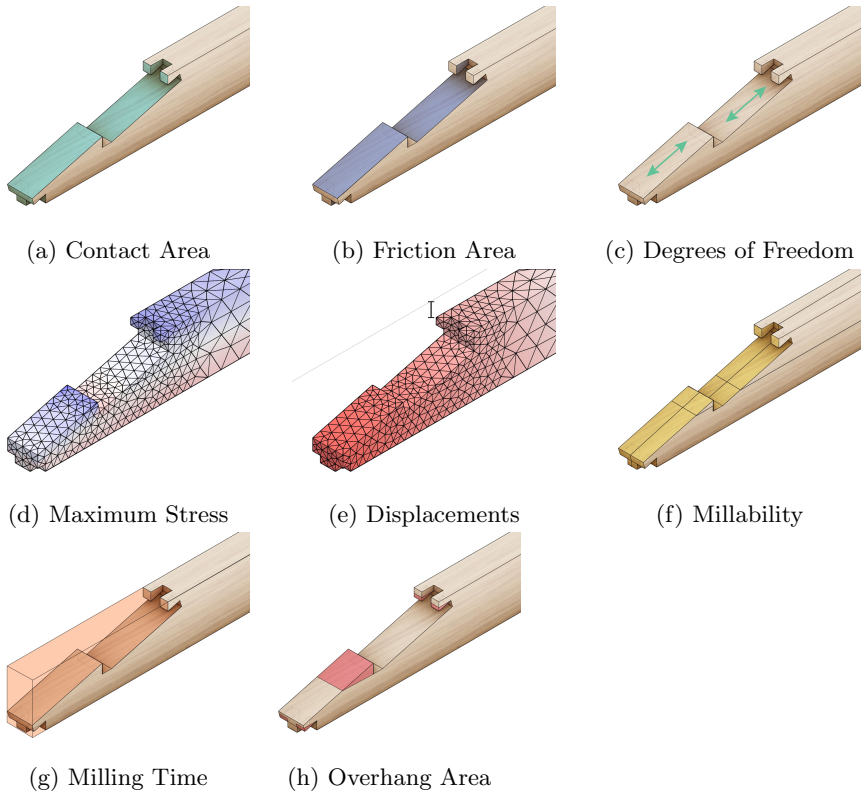
Figure 4.17: Each metric was gathered during the analysis steps to assess performance for the joint and create comparisons in a joint family.

Creating a series of comparable metrics facilitated trend finding for the benefits and limitations of each connection family. Using the data gathered from the previous steps, comparing seemingly disparate information reveals

commonalities. When looking through the data for both the structural and fabrication side, we picked key attributes used in literature as both geometric indicators and end-point metrics for performance. Along with these metrics, we also included many other metrics that we theorized would behave similarly to other metrics.

For geometric indicators, we speculated that the geometry of the assembly could be used to predict the structural performance of the assembly. As the forces of the assembly travel through the members via the contact surfaces between them, evaluating whether the different characteristics of geometry correspond with increases or decreases in structural or fabrication performance. These metrics could provide a general trend without requiring additional analyses.

While data for each metric stems from the individual nodes or faces in the geometry, the resulting metric included only one value. This reduction was performed to create more comparable data between the different permutations. Although this reduction of information removes valuable data, it allowed us to plot the different results and interpret the data to find general aspects for the provided parametric models, quickly finding properties that correspond with beneficial characteristics.

Contact Area

Contact area, Figure 4.17 (a), referred to the surface area in contact with other faces in the assembly and was gathered in assembly analysis. Each element pair in the assembly totaled its own contact area, with the resulting value being either an area for a selected pair or a total of all contact areas. We theorized that this could be used as a geometric indicator for the structural performance of an assembly as additional contact between elements could indicate an increase in distribution of forces.

Friction Area

Friction area, Figure 4.17 (b), referred to the portion of contact area whose face normals are perpendicular to the sliding direction of the assembly and was gathering in the assembly analysis. This metric used the sliding axis for each member and included contact faces if their normals were perpendicular to the sliding direction. Friction area could provide better insights into certain connection types, as many connection types utilize friction to resist bending or to transfer load. Friction area should be compared to the structural performance of the assembly to see if it can act as a

reliable indicator for performance.

Degrees of Freedom

The degrees of freedom, Figure 4.17 (c), referred to the axis in which the assembly was allowed to slide past one another. For this metric, a range of values for angles around each of the primary axes were used rather than vectors. The differences in the extremes could be measured to estimate how restricted the assembly was for each member. We assumed that a larger range for the degrees of freedom would correspond with a joint that is not as rigid and had more opportunities for movement. Rigid connections could perform better, allowing the assembly to function as one element.

Maximum Stress

We used maximum stress, Figure 4.17 (d), as an end-point metric to determine the strength of an assembly. Timber connections generally fail due to either crushing or splitting of the fibers. Knowing the magnitude and location of stress concentrations provides valuable information and acts as the primary metric for structural performance. We had several methods for defining the maximum stress in the assembly as listed in the structural analysis section to account for discrepancies in results across different simulations.

Maximum Displacement

The maximum displacements, Figure 4.17 (e), in the simulation acted as an indicator for both the stiffness in the assembly but not for the structural performance. While displacements did not have as large a role in evaluating structural performance, they could still be used when comparing simulated models to physical models. In contrast to stress, displacements did not tend to concentrate at a single point in the assembly and thus produced more reliable results. These metrics could also be used when determining sag on an assembly.

Millability

Millability, Figure 4.17 (f), used the fabrication approach set during the constraints and milling analysis sections to determine if the elements of the assembly had valid geometry for the fabrication process. For each face in the geometry, this metric ranked each face by its milling priority along

all milling directions. The millability metric not only indicated if the part could be milled as a whole, but also which faces could not be milled or which members would have inefficient faces. This metric could be used to filter out invalid geometries and parts that would require extensive milling times.

Milling Time

We used milling time, Figure 4.17 (g), as an end-point indicator for the viability of fabrication. This metric used the curves created during the curve milling process along with the depth of each cut to create a volume for the space to mill out. Cutting length gathered from the volume, which is divided by the depth per cut and the bit radius. Milling time can then be derived by applying a feedrate to the cutting length. When comparing the different timber assemblies together, fabrication time is one of the largest factors when determining cost. Because all assemblies in a connection family will have the same construction process and the same member size, milling time was determined to be the most reliable estimate for fabrication costs.

Overhang Area

Overhang area, Figure 4.17 (h), was used as a metric in the Tsugite Study [Larsson et al., 2020]. Larsson established overhang area as a metric called "Durability." This metric was used to indicate a weakness in the geometry. Because timber-only has one strong axis, if a portion of the geometry creates an overhang perpendicular to that axis, the geometry can shear along that axis. We surmised that geometries with larger overhang areas would tend to have weaker connections, providing more opportunities to shear. This metric used the overhang method described in the milling analysis section with a milling direction along the grain to find overhangs perpendicular to the grain. The area of the overhangs was summed together to establish the overhang area metric.

4.10   Framework Outcome

The framework functioned as a large feedback loop, using the computational tools to rapidly gather data and display the information to users and designers. These tools have been gathered together into a single interface. With this methodology put into practice, different designs could have immediate performance metrics associated with them, using some or all of the

analysis available in this framework. The framework also utilized a modular approach to its analysis and feedback. New analysis tool or methods of displaying data helped to make the framework more accurate and robust. Further tools could be added for other metrics such as fire resistance, acoustics, or seismic performance. Alternative displays could reveal additional information through the use of additional plot types. Furthermore, this modular approach lends itself to other forms of development, such as GAs or other types of computations design models.

Chapter 5

Case Study

As a means to test the framework we used a series of case studies to investigate how effective this data driven approach would be for finding the right design space for a specific connection. We constructed two case studies to test different aspects of the tool. The first case study focused on the manufacturing side, using a CNC machine to mill parts and compare them to the simulated model, allowing us to calibrate and verify the results. The second case studied used these results to simulate larger members, such as ones typically found in mass timber construction. With this case study, we used a much larger design space, looking at a wide variety of permutations, but skipped the physical testing due to the limits of our fabrication shop.

For the design of the connection itself, we selected a scarf joint as it is a good candidate for timber joinery. The scarf joint only requires two members and a wedge, can generally be milled with a 3.5 Axis CNC machine, and provides an end-of-life use for reclaimed timber. The scarf joint has traditionally been used as a way to extend beam lengths prior to lamination and steel mechanical fasteners. The scarf joint typically consists of an angled cut along the vertical side of the member with a wedge placed in a hole in the middle of the joint. These connections typically have a vertical section at the end of the joint region called a shoulder with an interlocking blade keeping the assembly together. Historically, these connections tended to be used closer to a support. In order to simplify the model, we placed the connection in the center of the beam assembly to test the connection without any shear.

5.1 Parametric Model

a. Face-halved scarf
b. Side-pegging
c. Peg
d. Face-pegging
e. Face
f. Splayed scarf
g. Side
h. Side-halved
i. Vertical butt
j. Face-halved and bladed scarf
k. Squinted butt inside halved scarf
l. Undersquinted butt in halved scarf
m. Sallied butt
n. Through-splayed and tabled scarf
o. None
p. Side-halved and bridled scarf
q. Stop-splayed scarf
r. Key
s. Stop-splayed scarf with bridled butts and face key
t. Stop-splayed and tabled scarf with key
u. Through-splayed and tabled scarf with face key
v. Stop-splayed and tabled scarf with sallied and undersquinted butt, internal tongues and key

Figure 5.1: Traditional Scarf Joint characteristics and terminology (Vernacular Building Architecture Group)

For both test cases, we developed the same parametric model, with different constants for each of the case studies. When looking at how to design the parametric model, we studied existing features and terms from traditional scarf joints to create the variables and constants. Existing literature for scarf joints describe a series of terms for the family of scarf joints that are shown in Figure 5.1. In order to narrow down the number of variables in the scarf joints, we conflated many terms for similar concepts down to a series of variables that control the geometry of the connection. As can be seen below, we classified the parts of the scarf joint typology from the common terms for each section. A scarf joint consists of five different sections that work together to resist the moment connection: the scarf, the shoulder, the blade, the table and the bridle. Each of these sections has a set of properties that determine how it is formed as can be seen in Figure 5.2.

As the member needed to remain the same size for functional equivalence, the member height, width, and depth all form a set of constants that could

51

change for each of the sets of tests. Similarly, the location of the load for the structural analysis needed to remain constant across all sets in a test. The geometry of the connection itself was controlled by parameters and formed the variables for the case studies. For the simplicity of the case studies we restricted any variable that did not have a granular range such as the "number of tables" variable and the blade angle variables.

The variables themselves were created with set ranges that would function within the parametric model. We created the parametric model to encompass the majority of the design space within the connection family from only a small set of variables. The individual variables along with their range and descriptions are listed below.

5.1.1 Scarf Joint Typology and Variables
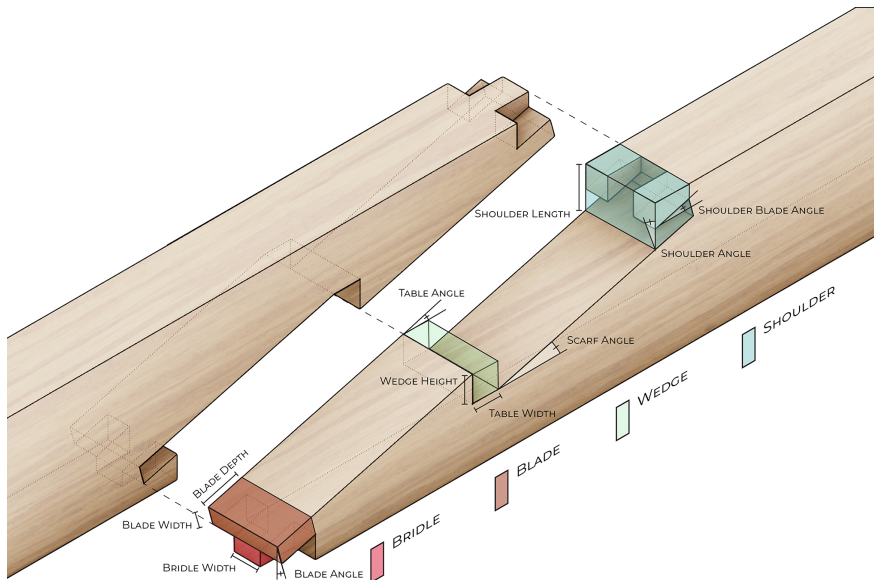
Figure 5.2: Scarf Joint Components and Variables. Most Joints within the Scarf Joint Family can be created using these sets of variables

Scarf   In a traditional scarf joint, the scarf defines the primary angle that the joint relies upon. Shallow angles allow for larger joints. The variables in this region is the scarf angle.

Shoulder   Along the edge of the joint, the shoulder usually defines the region that restricts the scarf and prevents it from sliding. This section also generally houses any blade or bridle. The variables in this region are the shoulder angle which defines the angle of the stop and the shoulder-length which in turn affects how large the shoulder, the blade, and the bridge can be.

Blade   Inside the shoulder, the blade runs along the scarf and digs into the shoulder, creating a locking mechanism. The variables in this region are the blade length, the blade width, as well as the angles along the top and the side of the blade.

Bridle   This section forms the tongue on the top of the joint at the shoulder. This prevents the joint from slipping laterally. The variable controlling this region is the bridle width.

Table, Key, or Wedge   The table generally houses the key or wedge placed in the scarf and gives the joint the standard 'lightning bolt' shape. The region contains the variables that affect the width and height of the keys or wedges as well as the angle that key is rotated.

5.1.2   Structural Setup

The structural setup for both the physical test and the mass timber test utilized a standard four point load setup as can be seen in Figure 5.3. Loading it with two supports and two loads located in the center of each of the beams would allow for simple bending to be tested without introducing shear into the joint region. This was used to keep the analysis and evaluation of the model simple. The loads for each of the different case studies was unique, but would be a percentage of the load for a solid beam of equivalent size. Further explanations about the loads and the supports for the typical setup can be found in the Methodology section on page 32.

(a) Physical Setup

(b) Bending Moment

(c) Shear
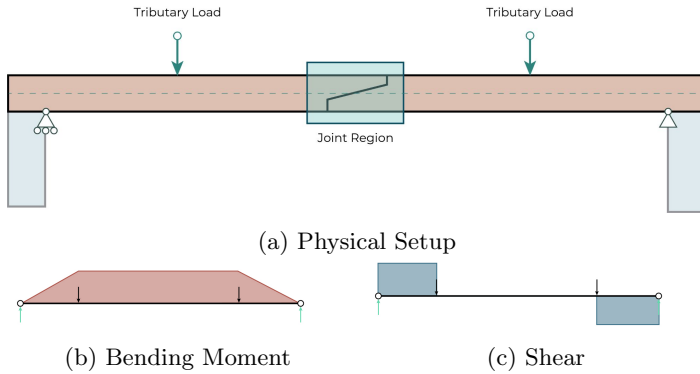
Figure 5.3: The physical testing setup. The setup includes tributary loads, and supports.

5.1.3 Initial Single Variable Simulation

Due to the high number of variables in scarf joint typologies, we performed an initial study to determine what variables contributed most to the performance landscape. Each variable was given a set range and a default value and was tested using the same boundary conditions. The results can be seen in Figure 5.4. After sorting the variables by variance, a set of variables stood out as affecting the performance of the assembly the most: scarf angle, shoulder-length, table angle, table length, and wedge width. While this initial test only covered a small portion of the enormous design landscape, it gave a baseline indication for where to run additional tests. Due to the limited scope of the initial test, each variable was assumed to react similarly across the different fitness landscapes. Variables with high variance would have the largest impact on the performance and thus were selected for the next phase of testing.

5.2 Physical Douglas fir Testing

For the first case study, we used the parametric model of the scarf joint to construct physical models. We were limited by the size of the CNC machine for physical testing. The Laguna Smartshop 2 SUV had a 1.5 meter by 3 meter bed with a Laguna Rotary Fourth Axis Attachment and could produce anything smaller than a 15 cm radius. This allowed us to mill almost any
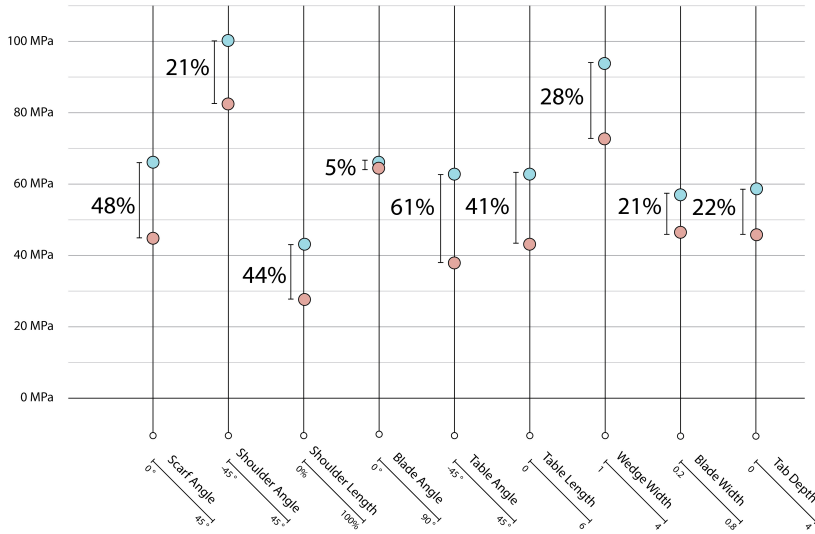
Figure 5.4: Initial Variance test for each variable. The maximum stress for each step along the range was compared to find the resulting range and variance percentage.

form of timber joinery without requiring additional manipulations by the machinist, as that would introduce errors in the accuracy and limit the precision of the contact faces. In order to further reduce errors in machining, the CAM for the part only reached halfway into the material, as longer bits tend to introduce inaccuracies. For the testing, we made a series of assumptions. We assumed that the assembly would rest at the center of a beam, with the beam itself being 3 meters long, 10 cm wide, and 10 cm deep. The beam would be first loaded with a 2 kN force at 0.75 meters and 2.5 meters. Once the base loading was complete, the beam would be milled to form the assembly using 3-axis operations across the 4 orthogonal rotations. We performed an initial study using a solid member in order to obtain the material properties as described in the Methodology section with a maximum allowable stress of 13.8 GPa.

From performing the initial setup studies, we discretized the mesh using different mesh densities as can be seen in the methodology section in Table 4.1. We found that at the resolution of 6 cm for the outer region, 2 cm for

Figure 5.5: The analogue indicator could gather measurements with a precision of up to 30 micrometers.

the inner region, and 0.75 cm for the contact area provided a consistent and accurate result from the FEA model. For the forces applied to the model, we assumed a baseline of 25% capacity for the connection and applied a force of 500 kN distributed along the points located at 0.75 meters and 2.25 meters. We compared the results of the simulation by comparing the maximum displacements and stresses from the model. Comparing the physical tests themselves, we focused on the displacements, as we were only able to gather the displacement and the critical load values when performing physical tests.

5.2.1 Control Beam Results
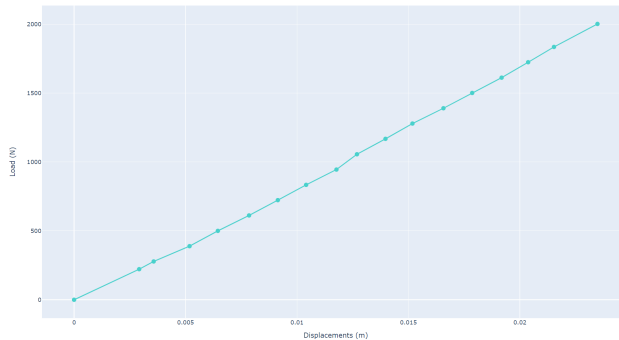
Figure 5.6: Load and Displacement table for a solid Douglas fir beam tested with the face grain facing horizontally and the edge grain facing vertically.

When measuring the deflection of the solid beam as the control, we measured the center point at the bottom of the beam using the analogue dial indicator as can be seen in the Figure 5.5. For each load case, we measured the maximum displacement on Table 5.6. From this, we can see a linear correlation between the load and the deflection of the beam. This reflected the linear model that we constructed.

Optimizing Materials from Results

Properties	Literature Properties	GA Properties
Elastic Modulus X	11 GPa	7.739 GPa
Elastic Modulus Y	0.4 GPa	0.559 GPa
Elastic Modulus Z	0.7 GPa	0.929 GPa
Poisson Ratio XY	0.535	0.535
Poisson Ratio YZ	0.419	0.419
Poisson Ratio XZ	0.019	0.019
Friction	0.5	0.5
Density	498 kg/m^3	498 kg/m^3
Allowable Stress	13.8 MPa	13.8 MPa

Table 5.1: Material Properties for Douglas fir before and after the GA

To maintain accuracy of material properties for timber without rigorous material testing, we decided to utilize a Genetic Algorithm or GA to match the simulation and the measured displacements on the physical tests. We used a package within COMPAS that included a generational GA for the optimization process [Mele and many others, 2021]. The variables that govern the inputs for the GA were a range of values for the three elastic moduli, ranging from 50% below to 50% above the value found in literature for Douglas fir. For the fitness function, we used the displacements measurements from the physical tests and subtracted them from the maximum displacements from simulated results for a beam of the same size with the same set of loads. The difference percentages were then averaged for a fitness value that represented the accuracy across several loads. The GA was run for 50 generations with 25 population in each generation. After using the GA to test different material properties, we found a set of material properties listed in the Table 5.1 that matched the maximum displacements, differing by only 0.0003%. From this we were able to create a simulation for the scarf joint tests that would more accurately depict the state of the connection.

5.2.2 Physical Test Simulation Results
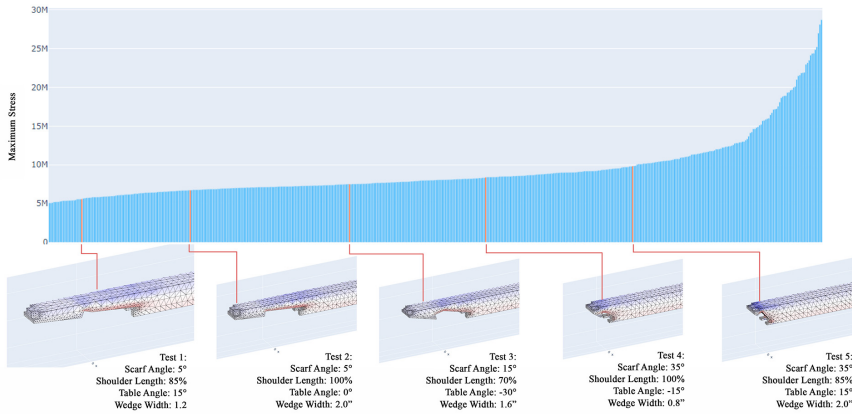
Figure 5.7: Graph plotting each of the permutations along the x-axis. The plots were sorted by the maximum stress in the FEA simulation. Five tests were selected at roughly 20% increments, with fabrication restrictions taken into account.

In addition to testing material properties, the case study was also used to ascertain whether increased performances in the simulation correspond to the physical tests. A rudimentary test was performed in order to create a large fitness landscape. Four variables were selected with five variations for each variable, creating a test with 625 permutations. The variables that were selected are displayed in Table 5.2 with the selected ranges. We surmised that these variables would produce a high variance in results while retaining their ability to be easily milled.

Once the analysis was completed for the dataset, we sorted the entire dataset of permutations by the maximum stress after 1% culling. The result was a graph that showed the permutations with the lowest stress to the highest, with a difference in stress of 25 MPa between the highest and lowest performing permutations. While these stress calculations did not predict the actual load capacity of the members, we predicted that they would perform proportional to the stress calculation. Once the permutations were sorted we could find five permutations at set percentiles. We selected five permutations to be tested using the physical testing setup as can be seen in Figure 5.7. The tests were selected at roughly 20% increments, restricted by millability

Variables	Range	Number of Steps
Scarf Angle	15° to 45°	5
Shoulder Length	40% to 100%	5
Table Angle	-45° to 45°	5
Table Length	0.4" to 2.0"	5
Wedge Width	1.0"	
Shoulder Angle	0°	
Blade Depth	40%	
Blade Width	40%	
Bridle Width	35%	

Table 5.2: Selected Ranges and number of steps for each variable

and total joint size.

5.2.3 Physical Test Process

Each of the five permutations were milled and cut using the milling curve creation tool and were cut with the same methods, machine, and with a 3/8 inch end mill. For each of the permutations, similar grain directions for the Douglas fir 10 cm by 10 cm posts were selected, with the face grain facing vertically and the edge grain facing horizontally. This was done to limit the need for the additional weight the stronger grain direction would require. The framework created the curves for each permutation as described in 4.7 to create a series of curves for pocketing operations. A process was created using RhinoCAM's API to automatically create G-code for the 4-axis machine operations milling out each pocket for a side and then rotating the part by 90 degrees. In order to keep the part on the 4 axis machine, a part of the stock was left with cut off markers for a manual removal as can be seen in Figure 5.8.

The keys in each assembly were constructed as two 3d printed wedges with scrap material in between to account for the differences in key sizes. This was done, both to verify that the wedge was not contributing to the performance and to reuse the same key across multiple assemblies regardless of key size. Each member was finished by hand and used the same setup for physical testing.

The physical testing rig utilized two supports on each side, spaced 6 meters apart with a set of weights on each end to prevent movement. The analogue indicator was mounted on a separate scaffolding to prevent movement from the assembly affecting the measurements. The four point loading

Figure 5.8: Image of 4-axis milling process. A part of the stock was left to continue milling across each of the four axes.

system utilized two palettes along with rigging straps. We placed additional weights on each side to create a baseline 222 N for the tests. For each permutation, an increasing load at 45 N increments we placed on the palettes. We measured the displacements once the applied load was stabilized. Once the displacements exceeded 2 cm, the indicator was removed and the load was incremented until the assembly reached its critical load and failed. The results for the five tests can be seen in the Figure 5.9.

5.2.4   Physical Test Results

When observing the results, the resulting displacements from the five physical tests follow a linear deflection in relation to the increased load, which was expected for the members prior to plastic deformation. While the displacements measured in the physical test could not be compared to the stress received during the simulation, the critical loads for each of the
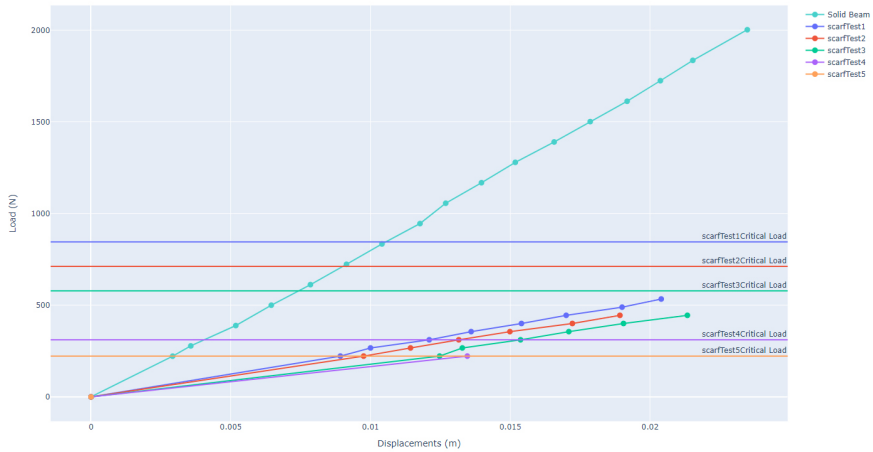
Figure 5.9: Graph plotting the displacements of the selected permutations in Figure 5.7. The measured displacements trend similarly to the expected performance.

permutations trended similarly to the maximum stress ratios for the simulations. A high performing permutation in the simulation seemed to predict a high degree of performance in the physical test. This supports our methods for analysis and data manipulation of the simulated assemblies. Although the method can indicate relative performance, it would be inappropriate to use the results as a predictor for what load the failure will occur at, as the failure criteria for timber is much more complicated than measuring the maximum stresses.

5.3 Mass Timber Simulation

In addition to rapidly prototyping the physical connections, one advantage to a computational model is the ability to perform numerous analyses to obtain a high performing result across different requirements. The computational analysis can not only run all the different forms of analysis, but can also determine if each permutation meets the base requirements for the assembly. Once the analysis is run for each of the permutations, a fitness landscape displays the relevant information to the user, allowing them to decide on the optimal solution based on the disparate results from the analysis.

In order to test these ideas, we will be using a case study for recycled mass timber, as this sort of analysis would need to be performed to understand how timber joinery would function as a proposed method for re-use.

5.3.1 Setup

Similar to the first case study, this analysis used the scarf joint parametric model in order to test the framework, with the members being sized appropriately for a mass timber beam. The beams each measure 30 cm by 10 cm by 6.6 m with a support at 0.3 m and 6.3 m. This allows for a span of 12 m across the entire study. The load for the study are placed at one quarter and three quarters the assembly span with a total load of 2.6 kN distributed between them along a line perpendicular to the beam direction. This case study evaluated a series of spliced scarf joints for mass timber beam to beam connections. Due to fabrication constraints, this case study only simulated models to estimate performance rather than performing physical testing on mass timber elements. As such, we were not able to calibrate the simulated model's material with physical tests. We used material properties from literature [Vardaxis, 2014] as a baseline for the simulation. Additional physical testing could be performed using glue laminated beams to further calibrate this model and establish a closer estimate for the simulation. The material was determined to be a perfectly orthotropic material without glue layers, as the results from this study are intended for design decisions rather than definitive structural performance. The setup for the FEA model used the same boundary conditions. Similar to the physical test, the load was set to roughly one tenth the expected load for a solid member, as this helped simulations converge. As the FEA model only uses a linear elastic model for the analysis, the results are expected to be relatively proportional. Due to the change in member size, the test for the GMSH sizing was run again. The new sizes are listed in the methodology section in Table 4.2.

For the purposes of a fully simulated study, we designed a more granular design space, in order to identify trends along each of the variables. To achieve this granularity, we divided each of the top five variables into 17 steps as can be seen in Table 5.3. Rather than create a unique permutation for each of the sets, which would have resulted in 17^5 permutations, variables were paired together, allowing for a two-dimensional landscape to compare the variables together. This would still allow for comparisons between the variables while only requiring $17^2 * 10$ permutations. Ultimately, with this approach we were able to evaluate the role each variable had upon the metrics rather than just selecting the permutation with the best performance.

Variables	Range	Number of Steps
Scarf Angle	5° to 45°	17
Shoulder Length	20% to 100%	17
Table Angle	-30° to 30°	17
Table Length	1.0" to 5.0"	17
Wedge Width	1.0" to 5.0"	17
Shoulder Angle	0°	
Blade Depth	60%	
Blade Width	40%	
Bridle Width	35%	

Table 5.3: Selected Ranges and number of steps for each variable

5.3.2 Mass Timber Simulation Results

After running the simulation, 2790 of the 2898 permutations returned successfully, totaling a 96.3% success rate. The simulations returned with the stress and displacement values for each of the nodes in the model. Overall values such as maximum stress at each culling and smoothing value were also precalculated to allow for quick displays of all permutations. Combined with the other types of analysis, each of the remaining permutations could now be displayed and analyzed for trends. The observations can be found in Chapter 6.

Chapter 6

Discussion

While this study focused on evaluating the efficacy of a computational and data driven approach to joinery design, the results for the study come from the two case studies that focused on one connection family. As such, the results from the approach are limited by only having one set of data to refer to. Additional tests using other connection families would further the results and reinforce many of the claims created in this chapter while also finding parallels between different connection families and trends that exists between them.

The methodology for creating the observations for the results is telling in how effective the process was at understanding the inner workings of the geometries. Many dashboards were created to understand and compare the data between the different permutations. Dashboards that investigated stress distributions, plots between different analysis results and geometric indicators provided a robust method for understanding all forms of connections. These visual representations of joint characteristics provide useful tools for displaying and simplifying data between disparate fields with differing interests. This reinforces the tool as a form of pedagogy and as a communication tool for better decision-making.

6.1 Physical Testing Observations

When gathering data on the physical test result, we compared the simulated models to the displacements found on the physical results. The maximum displacement for each load for the simulated models behaved similarly

to the physical models with an error of around 10% across all simulations. While this different can be explained by the lack of additional testing of the physical results and the variances in the natural material, this also showed a limit to the efficacy of the simulation tool. By observing the results for the structural analysis, we could reliably compare different permutations to each other, but had a difficult time predicting performance. More work would need to be done to develop a tool that could act as a predictor, such as additional physical tests, a more robust FEA model, or addition material tests.

6.2 Edge and Face Grain Observations
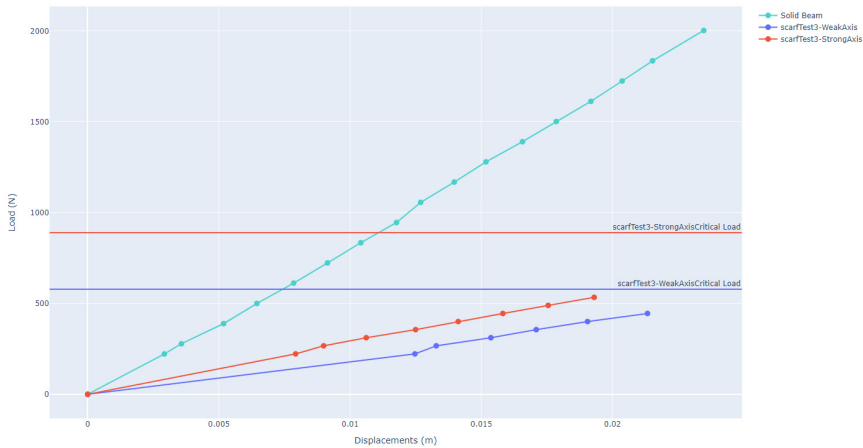
Figure 6.1: Graph displaying displacements of the same geometry with only the grain direction changing. The weak axis plot used the edge grain along the horizontal plane, while the strong plot used the edge grain along the vertical plane.

In relation to the physical tests, the geometry for permutation 3 was also tested to determine the effects for the different grain directions. When performing the GA for the solid beam, an elastic modulus of 0.559 GPa for the y-axis and 0.929 GPa for the z-axis were observed. We performed the same test for each grain direction. We observed that the assembly performed comparatively to the proportions of the elastic modulus along the different

axis. While additional physical testing would be needed to confirm the results, this observation does support our claim that using these series of computational tools allow designers to reach a rough approximation of the performance of an assembly as well as how to rapidly prototype solutions for increasing performance.

6.3   Mass Timber Simulation Results
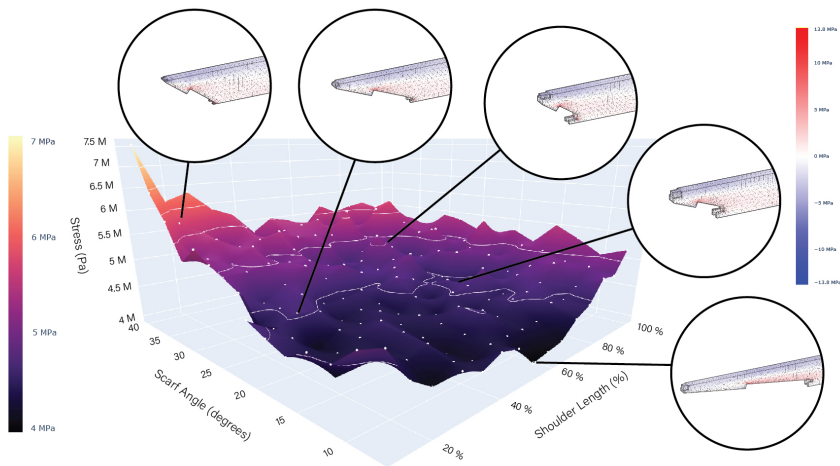
Figure 6.2: 3D Surface plot depicting the maximum stress (1% culled) for a series of permutations with the x-axis defining the change in scarf angle and the y-axis defining the change in shoulder-length. The stress for the plot utilizes the culling method described in the methodology section.

When evaluating the metrics for the large dataset, we first evaluated each pairing individually in order to find key takeaways. We used Plotly and Dash to create a series of dashboards to analyze the data. To analyze a pairing, we plotted the permutations along the x and y-axis, with the gathered response using the z axis. Using maximum culled stress condenses the information down so that trends between the different permutations become evident. As can be seen in the Figure 6.2, a clear trend exists across the fitness landscape. The dashboard created allowed for each permutation

to be selected and show the stresses on the geometry itself. This enabled further investigation as we could identify what caused high stresses across a landscape and create conclusions accordingly. A list of fitness landscapes can be found in Appendix A.

For the connection family selected in the Chapter 5, two location in the joint region continually failed for all geometries tested. Each concentration of forces could be abetted by studying how the different variables changed the geometry and the resulting stresses in the model.

(a) Blade Failure

(b) Low Performing Joint

(c) High Performing Joint
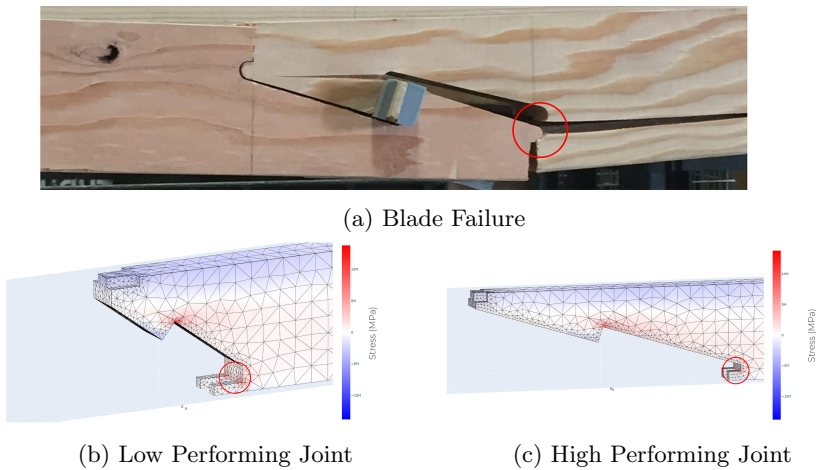
Figure 6.3: Diagrams illustrating the difference in the permutations from a low and high performing assembly for the blade stress concentration.

For instance, when evaluating the stress concentration around the lower blade in the scarf joint, we observed that certain variables affected this region more than others. The scarf angle and shoulder-length variables combined contributed the most to this region. We observed that there was a nadir at around 15 degrees for the scarf angle and at around 40% shoulder-length as can be seen in Figure 6.2. We surmised that the stresses in this region were caused by the beams wanting to rotate, with the two prongs on the shoulder holding the joint in place. A larger joint region caused more force to distribute across the entire joint region rather than being concentrated at the blade as can be seen in Figure 6.3. A larger shoulder increased the effectiveness of the shoulder from resisting the rotation and would prevent a stress concentration.
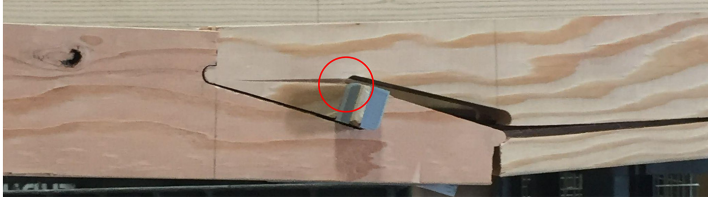
(a) Table Failure
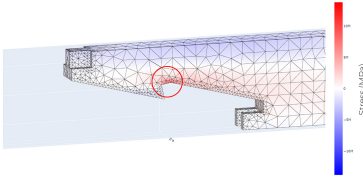
(b) Low Performing Joint
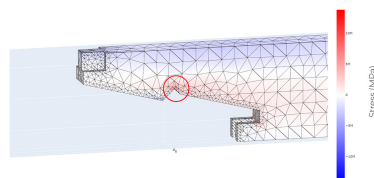
(c) High Performing Joint

Figure 6.4: Diagrams illustrating the difference in the permutations from a low and high performing assembly for the table stress concentration.

Similarly, the stress concentration around the table responded to changes in variables affecting that region. The table angle and wedge width variables affected this region the most. When evaluating both the simulations and the physical tests, we noticed that this stress concentration would tend to cause a shear failure at the table. Permutations that failed at lower stresses had less total area along the shear plane as can be seen in Figure 6.4. We assumed that the rotation of the table and the width of the wedge contributed the most in reducing or increasing this area and thus a table angle of 30 degrees and a small wedge width would minimize the stress in this area.

6.4   Stress Culling

Stress culling proved useful when sorting through the different permutations and comparing fitness landscapes. Without culling, permutations could have large variances in maximum stress with minimal changes in GMSH sizing, forces, or even geometry. Using a small degree of culling allowed for easier comparisons between permutations when compared to the Gaussian blur approach. A culling value of between 0.5 - 5 % produced less noisy results as can be seen in Figure 6.5. Values larger than 10% started
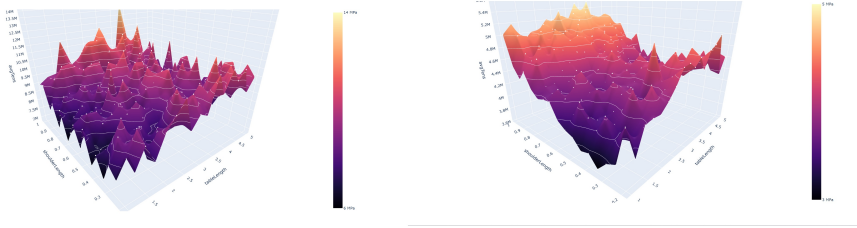
Figure 6.5: 3D Surface plot depicting the shoulder-length, table-length pairing. Left: 0% culling. Right: 2% culling.

introducing false positives as can be seen in the methodology section. As we developed a more refined and robust FEA model, the noise of the model drastically reduced. Further reductions in noise could be achieved by increasing mesh density and including additional load steps. However, adding more contact elements for the assembly tended to result in larger instances of non-convergence, limiting the efficacy of the process as a quick and efficient design tool. Because the process focuses on early design applications, the accuracy of the tool does not need to be as robust as other structural checks later in the design process. Due to this limitation, culling the stresses proved an effective solution; retaining accuracy for predicting performance while limiting simulation time. Because the culling value can be changed in the results section, part of the evaluation process for assessing performance included altering the culling percentage.

6.5 Stress/Displacement Comparison

While stress and displacement both correspond to the stiffness of the assembly and are related, they do not directly correspond to each other. As seen in Figure 6.6, there exists a trend for culled stresses and displacements, but when designing for each assembly, both will need to be evaluated and taken into consideration. Stress acts as a reliable indicator for performance but was difficult to observe and test when performing physical models. Displacements performed much better when representing stiffness and could be used both for code compliance and used in conjunction with physical testing. For this reason, both metrics were included in the final observations.
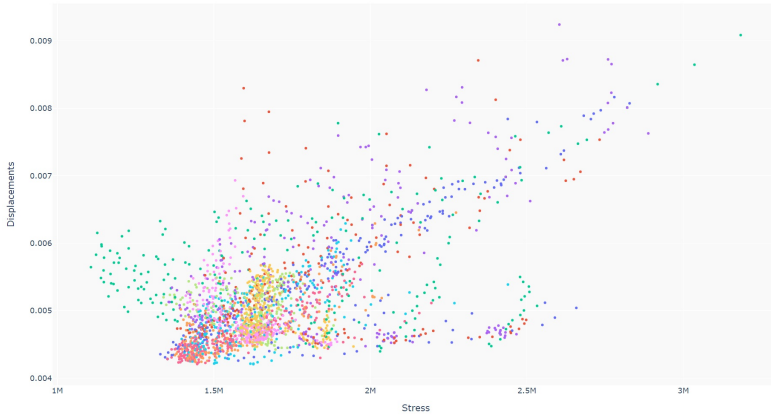
Figure 6.6: Plot comparing displacements to culled stress (10%) for all mass timber simulations. The color indicates which pairing the data was run in.

6.6 Geometric Indicators

Because the primary resistance strategy for integrated mechanical attachments is through geometry, we theorized that embedded information within the geometry could potentially point to high performance for a particular metric. We recorded the geometric indicators that were mentioned in previous literature to test this idea. Larsson et al. used contact area, friction area, and overhang area as measurements for performance in their study [Larsson et al., 2020]. While each connection family uses a different combination of factors to resist and transfer loads, the specific properties for each family are unknown.

Firstly, when comparing friction area and contact area, the two metrics were not statistically different from one another, with friction area only varying from contact area by around 5-10%. This was probably due to the connection family chosen, as there is not much difference between different scarf geometries and because friction does not play a large role in the functionality of scarf joints. As such, the analysis primarily focuses on contact area rather than friction area. Additionally, we observed that increases in contact area corresponded to increases in milling time. This was expected as larger connections would tend to have more surface area for the connection themselves, leading to longer milling times. This can be seen in Figure 6.7

When evaluating the relationship of these geometric indicators to the

70
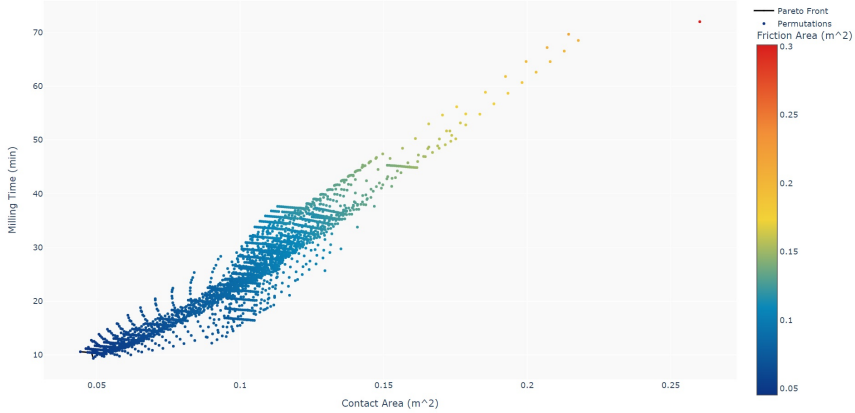
Figure 6.7: Plot showing the relationship between contact area, milling time, and friction area.

maximum stress, it was found that they did not directly relate to the performance. As can be seen in Figure 6.8, there does not seem to be a direct relationship between stress, contact area, and overhang area. As such, this does not seem to be a reliable predictor of structural performance. Observations of physical tests revealed that the shear area acted as a better analogue than the overhang area. We assume that different geometric indicators will have impacts upon performance in different scenarios. Metrics like friction area would have a much larger impact in structural setups that use friction as a factor in resisting forces. More metrics gathered from the geometry and structural scenarios would be needed to further evaluate the role of geometric indicators for structural performance.

The relationship between displacements and contact area yields more promising results, with an increase in contact area correlating to a decrease in displacements. We surmised that this potentially supports the idea that a larger joint region distributes the displacements over a larger area and thus reduces the maximum displacements. This is however not always the case, as some variable pairings saw an initial drop as contact area increased followed by an increase in displacements. Using the volume of the joint region could yield similar results with a larger correlation.

71

(a) Stress vs contact area plot with color as overhang area.
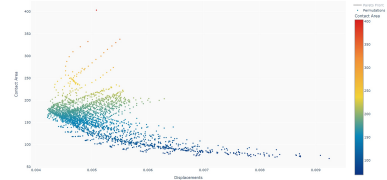
(b) Displacements vs contact area plot with color as overhang area.

Figure 6.8: Plots comparing different geometric indicators with stress and displacements. For the purposes of the scarf joint, these indicators did not have strong correlations

6.7 3D Pareto Front
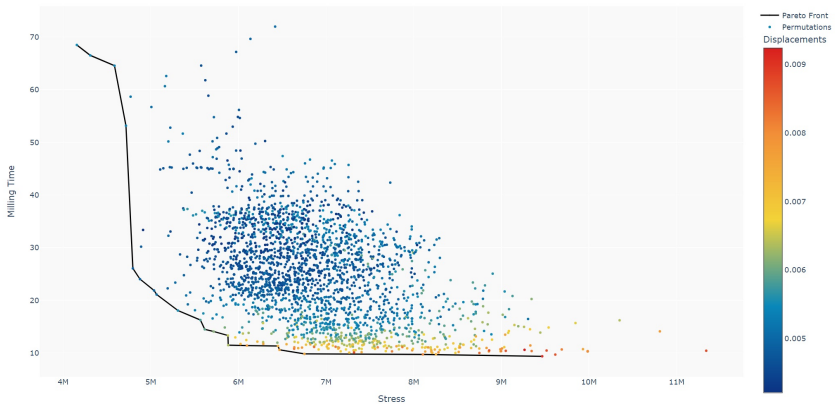
Figure 6.9: Pareto Front comparing Milling Time with Stress. The color describes the maximum displacement.

We utilized a standard Pareto plot to evaluate both the milling time and stress as the two gathered end-point metrics. Using the Pareto curve to display the best permutation for each ratio quickly produced good options for either fabrication, structure, or a combination of the two as can be seen in Figure 6.9. The overall Pareto front itself suggests that milling time and structural performance are not simply trade-offs and that there exists some geometry that can perform well in both regards, but that there is not

a single geometry that performs better than all others. This shows that specific geometry can be successful in maximizing performance regardless of structural or fabrication constraints, but that a wide range of geometries can be successful and be selected based on user preference or specific needs.

6.8 Scarf Joint Design Implications
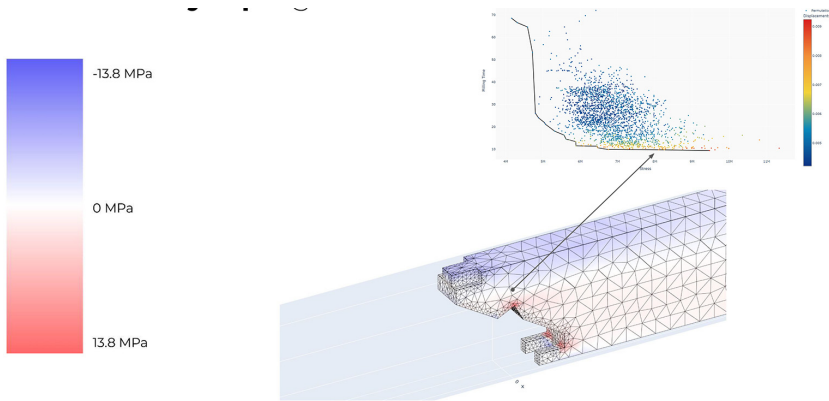
Figure 6.10: Permutation with low stresses but high milling time.

Using the Pareto front as a tool for designers, there are clear design solutions present depending on the requirements of the designer. For instance, if the designers have a high volume of timber with a low structural requirement, such as a short span, they could use a design such as the one seen in Figure 6.10 in order to minimize the milling times while still maintaining some structural capacity. The design uses large shoulder lengths with a steeper scarf angle in order to keep stress low while keeping the joint region as small as possible. Similarly, the table angle and size are rotated and minimized to keep the milling times down without large spikes in stress.

Alternatively if a designer is focused on creating as strong a connection as possible without regards to the milling time, a design closer to Figure 6.11 would be preferred. This design uses the largest joint region possible in order to distribute the loads across more of the beam. The shoulder and table lengths are maximized to further extend the size of the joint. This has the consequence of increasing the milling times dramatically, but this is less of a factor for a designer that would prioritize structure over fabrication.
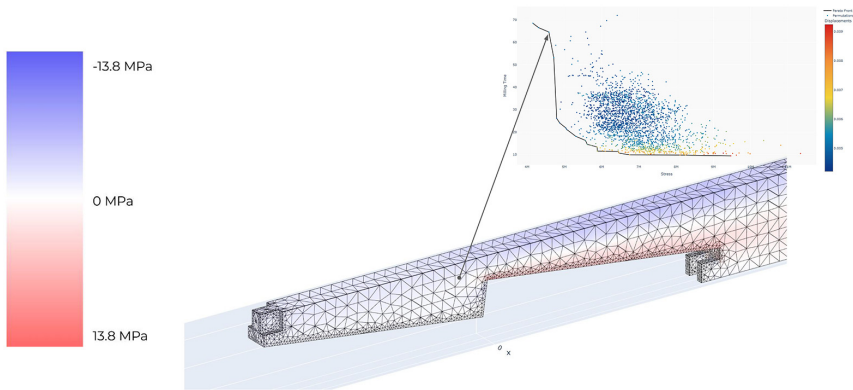
Figure 6.11: Permutation with low milling time but high maximum stress.

Finally, there exists designs that act as a jack of all trades, balancing different performance metrics to achieve a design that performs well overall. The design shown in Figure 6.12 acts similarly to the milling preferred design but allows for a slightly longer milling time to shore up weaknesses in stress. The design uses a shallower angle for the scarf and table to lower stress. Overall, these designs allow designers flexibility while weighing costs from different perspectives.

6.9   Framework Observations

While the framework offers advantages in evaluating designs quickly and can be used as a method for comparison, one of the major advantages present in the tool is the ability to compare disparate metrics together and find solutions that appease multiple fields. The built environment has many actors who each require different sets of values, making it difficult to find solutions that can cater to each. By having a system for comparing functionally equivalent connections, we can find options that present more than just trade-offs.

The ease of adding additional metrics also works to the framework's benefit. Other fields such as LCA studies, cost comparisons, and material volumes could be integrated and compared with little additional effort. Other comparisons such as species or concepts such as comparing solid sawn and mass timber could be created, creating comparisons between vastly different
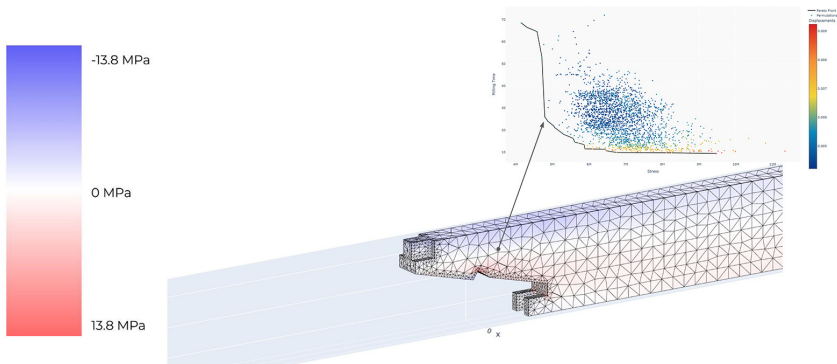
Figure 6.12: Permutation with considerations for both stress and milling time.

types of timber and providing additional persuading power for designers and contractors.

6.10 Limitations

This dataset was limited to only 0.2% of the total design space for the overall design for the scarf joints. While the pairing solution to the large design space created results that could be compared and spread out over a large part of the design region, there are significant parts of the design space that were not explored. We could have used an optimization algorithm such as simulated annealing to find the best results, but this removed the ability to test different variables and find trends when changing parameters in the parametric model.

Considerations for other metrics were also limited, as our focus was only on fabrication and structure. Because we were not focused on acquisition, the total member size or the effects that joinery would have on the number of pickups during construction was not considered.

In addition, only scarf joints were designed and tested using this framework. Without evaluating other design spaces and connection families, it is difficult to gather definitive conclusions about the framework. Additional testing on other geometric indicators and other families is needed in order to find a more broad understanding of timber joinery.

Chapter 7

Conclusion

This thesis revisits the work of traditional timber joinery through the lens of modern fabrication and analysis in order to address the potential limitations and benefits of timber joinery in modern construction processes. We proposed a framework to study the large variations in connection families and proposed methods to evaluate and compare different geometries, including assembly analysis, structural analysis, and fabrication analysis. To test the efficacy of our methodology, we developed a set of case studies using a scarf joint as a splicing connection between two beams. For the case studies we evaluated the efficacy of our methodology through accuracy with a physical case study and through data gathering through a simulated case study. The physical case study reinforced our confidence in the structural and fabrication metrics gathered through the analysis process. The simulated case study was used as a lens to determine if this would be a valuable approach for recommending certain design guidelines and rules of thumb for timber joinery. While more research would need to be done to create general guidelines, we observed that the data received from the analyses could be used for broad recommendations for a specific connection type. By utilizing large design spaces to evaluate trends, relationships could be drawn between different metrics from both fabrication and structural performance.

The overall design of connections can drastically affect the performance of the member itself across many fields. Having the ability to compare designs opens up discussions about different requirements and leads to more collaborations and innovations. By exploring these options through design early in the design process, we can resolve multiple issues at once. While

the exact nature of comparison and development can change, this process shows that exploring timber joinery design with a computational approach can present opportunities not present through other means.

7.1 Reflections

The study conducted provided a path for creating and testing different connection families, but was limited in scope. Further adjustments could be made to both improve the reliability of the study and include more use cases for the tool itself. A few of the potential improvements have been listed below.

7.1.1 Additional Geometric Indicators

The geometric indicators found during the study provided the first steps in creating alternative metrics to study timber connections, but additional metrics might lead to other discoveries for different connection families. During the study we found three geometric indicators: contact area, friction area, and overhang area. We also identified two additional metrics that could provide more accurate indicators for structural performance: shear area and joint region volume. More research would need to be performed to formally define these metrics and to test their efficacy, but it could lead to a better understanding of both specific connection families and underlying conditions for timber connections as a whole.

7.1.2 Structural Simulation

While wedges were included in the study, their effects were limited as they did not apply the forces typical to wedges. Typically, wedges will perform similar to prestressing the beam, increasing performance while keeping the connection tight. Wedges have been shown to have a significant impact on the performance of the joint. Loading the wedges prior to applying the tributary load in the FEA model could provide more accurate estimates for the simulation.

Additional work could also be done through the introduction of a more realistic model for FEA of mass timber. The laminate layers between the timber elements in mass timber are needed to create more accurate results. The significance of the laminate layers was not explored in this thesis and

could provide additional insights into its performance and potential weak spots.

Lastly, the structural simulations in this study only accounted for typical vertical load cases, using only live and dead loads. While studying the max stresses for typical vertical loads can yield valuable implications for design principles, additional testing with cyclic loading could provide other insights into the use case of timber-only connections after continued use and reuse. Additionally, lateral load testing could help to determine if integral mechanical attachments provide a benefit when dissipating energy in a seismic event.

7.1.3 Additional Physical Testing

The physical testing in the study only used rudimentary measurements and thus could only provide a limited amount of information. While critical load tests are valuable for the design and prototyping phase, further research is needed to help calibrate and verify the model. Additional testing with tools that measure the stress and strain of the material are needed in order to better understand the principal stresses and shear within the member prior to plastic deformation. More sensitive equipment or a larger number of tests could provide more accurate measurements across different members, as the members themselves can have varying material properties. This would give us a better understanding for how accurate the data was to the simulations.

7.1.4 Additional Use Cases

This research could be expanded to include uses for many of the new materials being created. CLT has become exceedingly popular, but there are still limited ways to connect the timber slabs together with the capabilities of resisting lateral loads without introducing additional steel elements such as timber seismic dampers. Historically, timber has performed well when resisting lateral loads in buildings. This is partly due to the lightweight nature of the wood, but could also be due to the flexibility of the material and the friction inside the connections and the allowance for small displacements within the connection. Using this tool in conjunction with additional FEA testing for lateral loads could point towards new connection types for mass timber panels. These connections could replace significant amounts of steel while preventing additional mechanical fasteners for CLT panels, thus promoting additional reuse benefits for vertical CLT systems.

Appendix A

Additional Plots
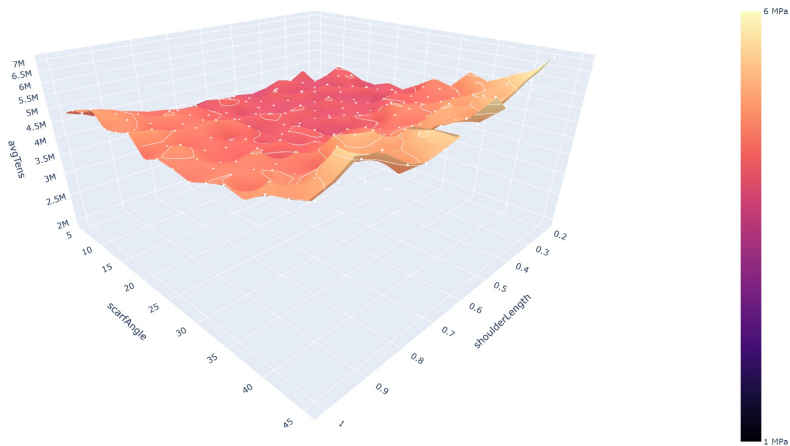
Figure A.1: Stress plot for Scarf Angle and Shoulder Length
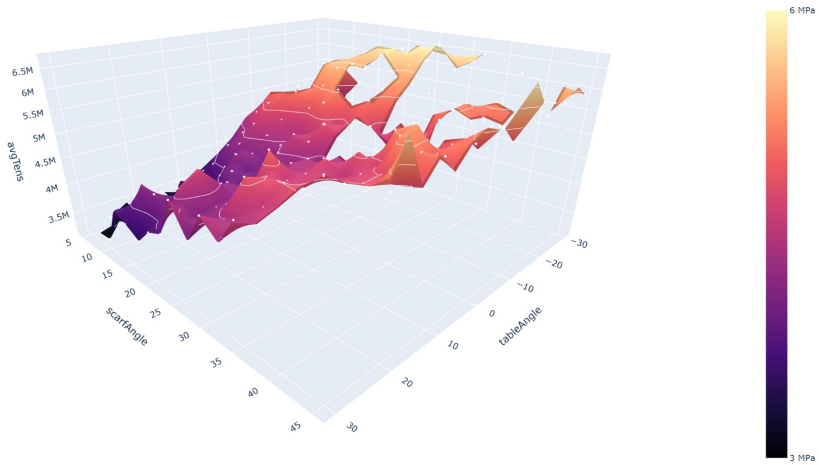
Figure A.2: Stress plot for Scarf Angle and Table Angle
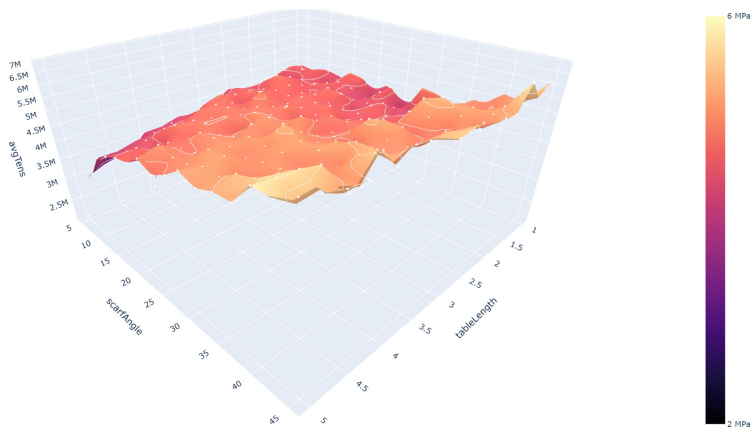
Figure A.3: Stress plot for Scarf Angle and Table Length
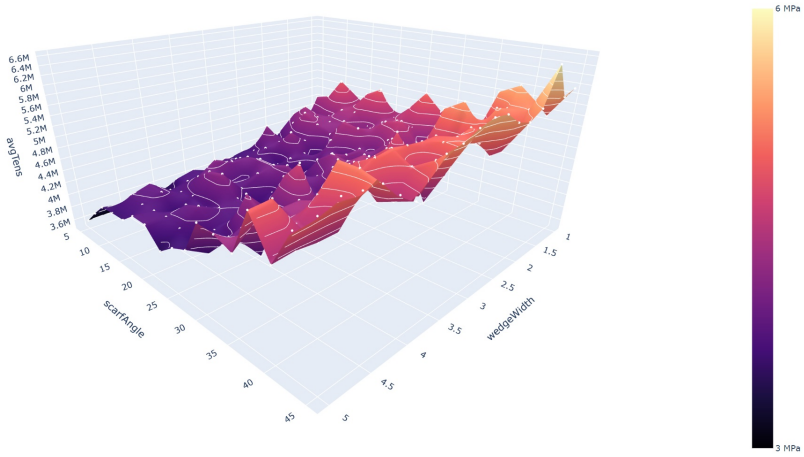
Figure A.4: Stress plot for Scarf Angle and Wedge Width
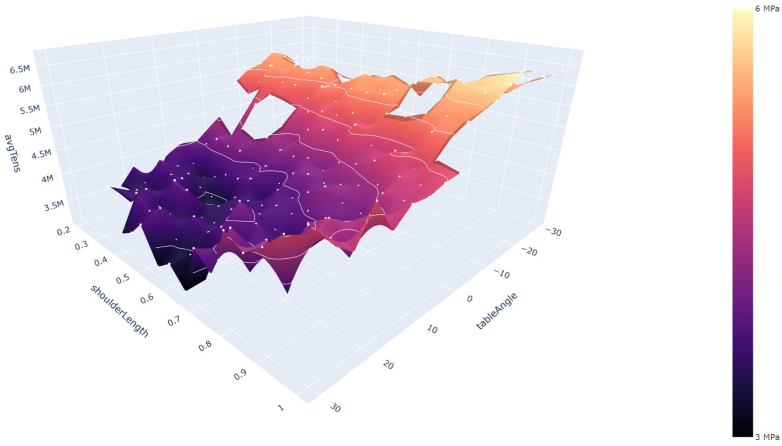
Figure A.5: Stress plot for Shoulder Length and Table Angle
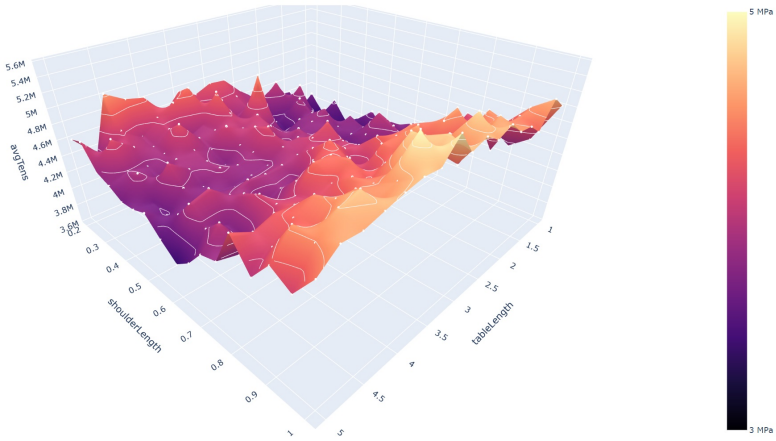
Figure A.6: Stress plot for Shoulder Length and Table Length
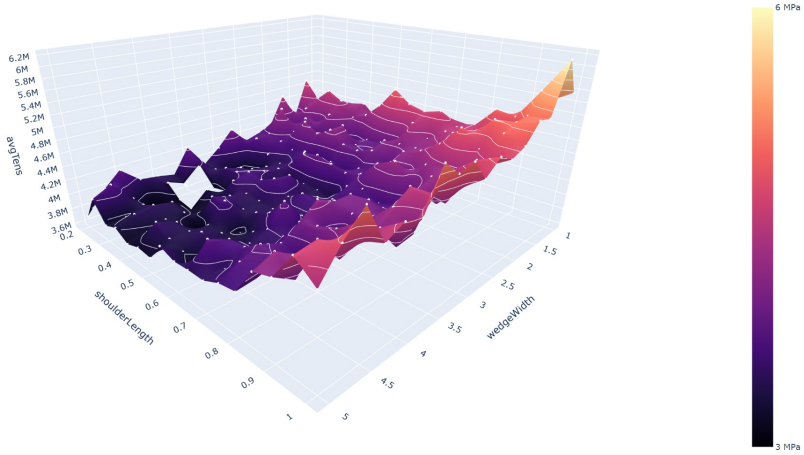
Figure A.7: Stress plot for Shoulder Length and Wedge Width
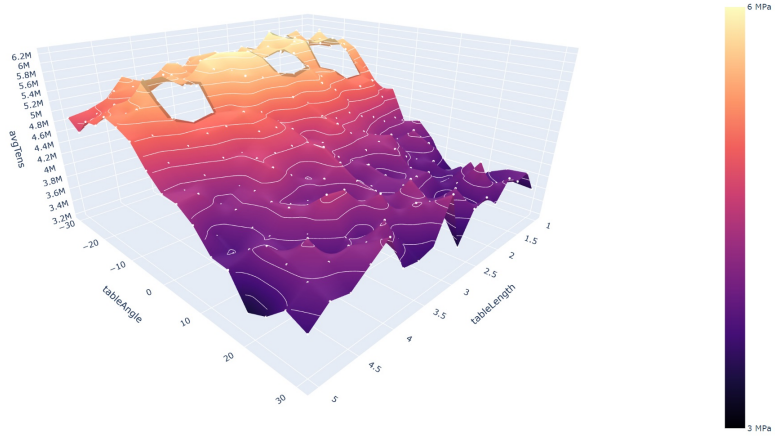
Figure A.8: Stress plot for Table Angle and Table Length
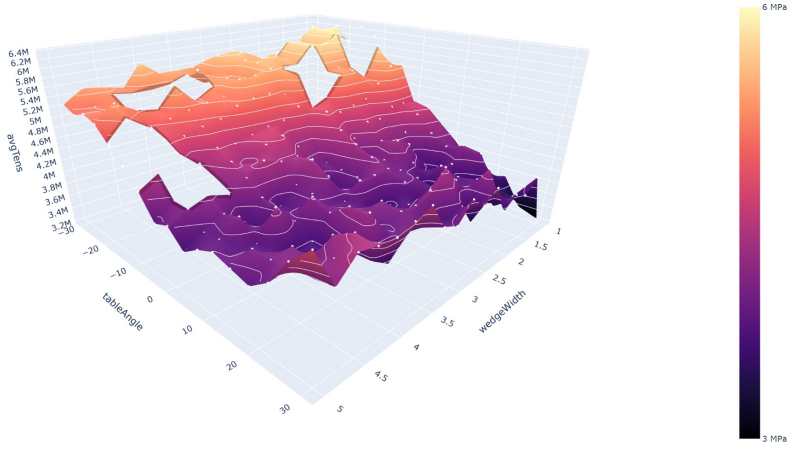
Figure A.9: Stress plot for Table Angle and Wedge Width
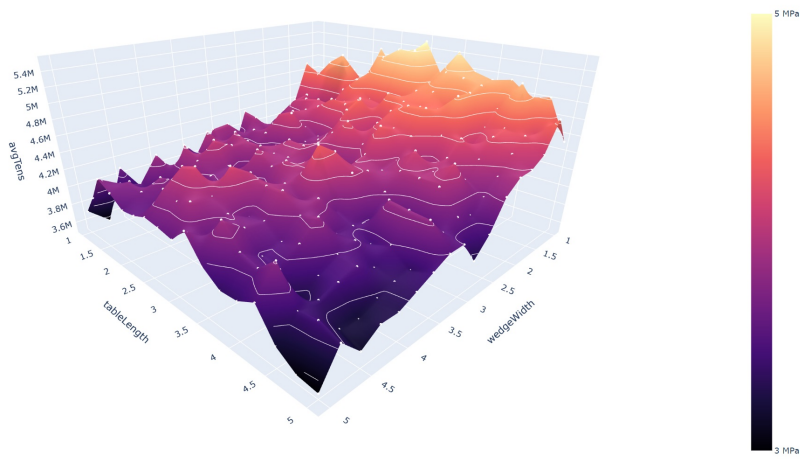
Figure A.10: Stress plot for Table Length and Wedge Width

List of Figures

Bibliography

[noa, 1973] (1973). Ise Shrine, Ise, JP.

[ver, 2023] (2023). Scarf Joint Typology.

[ACM SIGCHI, 2018] ACM SIGCHI (2018). Digital Joinery For Hybrid Carpentry.

[Adams, 1998] Adams, C. (1998). Japan's Ise Shrine and Its Thirteen-Hundred-Year-Old Reconstruction Tradition. *Journal of Architectural Education (1984-)*, 52(1):49–60. Publisher: [Taylor & Francis, Ltd., Association of Collegiate Schools of Architecture, Inc.].

[Architects, 2017] Architects, L. (2017). CLT Connection Prototype.

[Arciszewska-Kedzior et al., 2015] Arciszewska-Kedzior, A., Kunecky, J., Hasnikova, H., and Sebera, V. (2015). Lapped scarf joint with inclined faces and wooden dowels: Experimental and numerical analysis. *Engineering Structures*, 94:1–8.

[Arlet, 2021] Arlet, J. L. (2021). Innovative Carpentry and Hybrid Joints in Contemporary Wooden Architecture. *Arts (Basel)*, 10(3):64–.

[author/blaine brownell, 2016] author/blaine brownell (2016). A History of Wood and Craft in Japanese Design. Section: Technology.

[Brooks, 2015] Brooks, D. (2015). *Japanese wooden boatbuilding = Wasen*. Floating World Editions, Warren, CT. Book Title: Japanese wooden boatbuilding = Wasen.

[Brown, 2014] Brown, A. (2014). *The Genius of Japanese Carpentry: Secrets of an Ancient Woodworking Craft*. Tuttle Publishing, North Clarendon, UNITED STATES.

[Chen, 2019] Chen, C. X. (2019). Environmental Assessment of the Production and End-of-Life of Cross-Laminated Timber in Western Washington. page 193.

[Demattè et al., 2018] Demattè, M. L., Zucco, G. M., Roncato, S., Gatto, P., Paulon, E., Cavalli, R., and Zanetti, M. (2018). New insights into the psychological dimension of wood–human interaction. *European Journal of Wood and Wood Products*, 76(4):1093–1100.

[Echenagucia, 2020] Echenagucia, T. M. (2020). COMPAS Vibro: A framework for computational research in architecture and structures. https://github.com/Design-Machine-Group/compas_vibro.

[Fang, 2020] Fang, D. (2020). Timber joinery in modern construction: Mechanical behavior of wood-wood connections. page 144.

[Fang and Mueller, 2021] Fang, D. and Mueller, C. (2021). Mortise-and-tenon joinery for modern timber construction: Quantifying the embodied carbon of an alternative structural connection. *Architecture, Structures and Construction*.

[Fu et al., 2015] Fu, C.-W., Song, P., Yan, X., Yang, L. W., Jayaraman, P. K., and Cohen-Or, D. (2015). Computational interlocking furniture assembly. *ACM Transactions on Graphics*, 34(4):91:1–91:11.

[Geuzaine, Christophe and Remacle, Jean-Francois, 2020] Geuzaine, Christophe and Remacle, Jean-Francois (2020). Gmsh.

[Harte, 2017] Harte, A. (2017). Mass timber: the emergence of a modern construction material. *Journal of Structural Integrity and Maintenance*, 2:121–132.

[Kalisnekoff, 2021] Kalisnekoff (2021). 9-ply CNC Operation.

[Karolak, 2021] Karolak, A. (2021). Experimental investigation of timber beams with splice and scarf joints. *Construction and Building Materials*, 306:124670.

[Karolak et al., 2020] Karolak, A., Jasienko, J., Nowak, T., and Raszczuk, K. (2020). Experimental Investigations of Timber Beams with Stop-Splayed Scarf Carpentry Joints. *Materials*, 13(6):1435. Number: 6 Publisher: Multidisciplinary Digital Publishing Institute.

91

[Kindratsky, 2023] Kindratsky, M. (2023). Seedlings to solutions: Efficient resource use in mass timber manufacturing. In *Seedlings to Solutions*.

[Kretschmann, 2010] Kretschmann, D. E. (2010). Mechanical Properties of Wood.

[Kunecky et al., 2015] Kunecky, J., Sebera, V., Tippner, J., Hasnikova, H., Kloiber, M., Arciszewska-Kedzior, A., and Milch, J. (2015). Mechanical Performance and Contact Zone of Timber Joint With Oblique Faces. *Acta Universitatis Agriculturae et Silviculturae Mendelianae Brunensis*, 63(4):1153–1159.

[Kunic, 2021] Kunic, A. (2021). Design and assembly automation of the Robotic Reversible Timber Beam. *Automation in construction*, 123.

[Kuroishi, 2014] Kuroishi, I. (2014). Mathematics of Carpentry in Historic Japanese Architecture. In *Architecture and Mathematics from Antiquity to the Future*, pages 333–347.

[Langum et al., 2009] Langum, C. E., Yadama, V., and Lowell, E. C. (2009). Physical and Mechanical Properties of Young-Growth Douglas-Fir and Western Hemlock from Western Washington.

[Larsson et al., 2020] Larsson, M., Yoshida, H., Umetani, N., and Igarashi, T. (2020). Tsugite: Interactive Design and Fabrication of Wood Joints. In *Proceedings of the 33rd Annual ACM Symposium on User Interface Software and Technology*, pages 317–327, Virtual Event USA. ACM.

[Lopes, 2007] Lopes, D. M. (2007). *Shikinen Sengu* and the Ontology of Architecture in Japan. *Journal of Aesthetics and Art Criticism*, 65(1):77–84.

[Mackerle, 2005] Mackerle, J. (2005). Finite element analyses in wood research: a bibliography. *Wood Science and Technology*, 39(7):579–600.

[Magrisso et al., 2018] Magrisso, S., Mizrahi, M., and Zoran, A. (2018). Digital Joinery For Hybrid Carpentry. In *Proceedings of the 2018 CHI Conference on Human Factors in Computing Systems*, pages 1–11. Association for Computing Machinery, New York, NY, USA.

[Mehra et al., 2021] Mehra, S., O'Ceallaigh, C., Sotayo, A., Guan, Z., and Harte, A. M. (2021). Experimental characterisation of the moment-rotation behaviour of beam-beam connections using compressed wood connectors. *Engineering Structures*, 247:113132.

[Mele and many others, 2021] Mele, T. V. and many others (2017-2021). COMPAS: A framework for computational research in architecture and structures. http://compas.dev.

[Messler, 2006] Messler, R. W. (2006). *Integral mechanical attachment: a resurgence of the oldest method of joining.* Butterworth-Heinemann, Burlington, MA. Book Title: Integral mechanical attachment : a resurgence of the oldest method of joining.

[Moradei et al., 2018] Moradei, J., Brütting, J., Fivet, C., Sherrow-Groves, N., Wilson, D., Fischer, A., Ye, J., and Cañada, J. (2018). Structural Characterization of Traditional Moment-Resisting Timber Joinery. page 8.

[Nakashima, 1981] Nakashima, G. (1981). *The soul of a tree: a woodworker's reflections.* Kodansha International, Tokyo ; New York, 1st ed. edition. Book Title: The soul of a tree : a woodworker's reflections.

[Noeckel et al., 2021] Noeckel, J., Zhao, H., Curless, B., and Schulz, A. (2021). Fabrication Aware Reverse Engineering for Carpentry. *Computer Graphics Forum*, 40(5):301–314.

[Patalas et al., 2022] Patalas, F., Karolak, A., and Nowak, T. P. (2022). Numerical analyses of timber beams with stop- splayed scarf carpentry joints. *Engineering Structures*, 266:114626.

[Rezaei Rad, 2020] Rezaei Rad, A. (2020). *Mechanical Characterization of Integrally-Attached Timber Plate Structures: Experimental studies and macro modeling technique.* Doctoral Thesis, ETH Zurich. Accepted: 2021-04-07T15:39:58Z.

[Robeller, 2014] Robeller, C. (2014). Interlocking Folded Plate: Integrated Mechanical Attachment for Structural Wood Panels. In *Advances in Architectural Geometry 2014*, pages 281–294.

[Robeller, 2017] Robeller, C. (2017). Integral joints for timber folded plate structures. In *Advancing Wood Architecture*, pages 73–85.

[Robeller, 2019] Robeller, C. (2019). Timber Plate Shell Structures: A Digital Resurgence of Traditional Joining Methods. In *Digital Wood Design*, pages 1117–1133. ISSN: 2366-2557.

[Rogeau et al., 2021] Rogeau, N., Latteur, P., and Weinand, Y. (2021). An integrated design tool for timber plate structures to generate joints geometry, fabrication toolpath, and robot trajectories. *Automation in Construction*, 130:103875.

[Sangree and Schafer, 2009] Sangree, R. H. and Schafer, B. W. (2009). Experimental and numerical analysis of a stop-splayed traditional timber scarf joint with key. *Construction and Building Materials*, 23(1):376–385.

[Seike, 1977] Seike, K. (1977). *The art of Japanese joinery.* JWeatherhill, New York, first edition. edition. Book Title: The art of Japanese joinery.

[Shao et al., 2020] Shao, B., Lewis, N., Fischer, A., Huang, Y., and Lancelot, F. (2020). Parameters Identification for Wood Material (*MAT_143) and its Application on the Modeling of a Typical Timber Nuki Joint. page 16.

[Song et al., 2017] Song, P., Fu, C.-W., Jin, Y., Xu, H., Liu, L., Heng, P.-A., and Cohen-Or, D. (2017). Reconfigurable interlocking furniture. *ACM Transactions on Graphics*, 36(6):174:1–174:14.

[Stamets, 2011] Stamets, J. (2011). Bullitt Center Connections.

[Timber, 2015] Timber, Q. (2015). Softwood Microstructure.

[TimberLabs, 2022] TimberLabs (2022). Heartwood Connection.

[Vardaxis, 2014] Vardaxis, N.-G. (2014). Finite Element Modelling for Cross Laminated Timber Constructions. page 75.

[Varju, 2009] Varju, H. (2009). Cutting edge woodworking. *Canadian home workshop*, 32(3):14–.

[Woodworks,] Woodworks. Do wood-frame buildings need to account for thermal movement?

[Yang et al., 2008] Yang, T.-H., Wang, S.-Y., Lin, C.-J., and Tsai, M.-J. (2008). Evaluation of the mechanical properties of Douglas-fir and Japanese cedar lumber and its structural glulam by nondestructive techniques. *Construction and Building Materials*, 22(4):487–494. Publisher: Elsevier B.V.

[Zhang, 2022] Zhang, C. (2022). *Design for a Reconfigurable Mass Timber Building System.* M.Arch., University of Washington, United States – Washington. ISBN: 9798837533013.

[Zhao et al., 2021] Zhao, H., Willsey, M., Zhu, A., Nandi, C., Tatlock, Z., Solomon, J., and Schulz, A. (2021). Co-Optimization of Design and Fabrication Plans for Carpentry. *arXiv:2107.12265 [cs]*. arXiv: 2107.12265.